T.R.
ONDOKUZ MAYIS UNIVERSITY
INSTITUTE OF GRADUATE STUDIES
DEPARTMENT OF NANOSCIENCE AND NANOTECHNOLOGY

DIFFERENTIAL GENE EXPRESSION ANALYSIS OF *CANDIDA ALBICANS* EXPOSED TO BIOLOGICALLY-SYNTHESIZED SILVER NANOPARTICLES

Master's Thesis

Osaid ALHAROUN

Supervisor

Assoc. Prof. Dr. Hilal AY

This thesis was supported by Ondokuz Mayıs University with project number PYO.FEN.1904.22.015

SAMSUN
2023

ACCEPTANCE AND APPROVAL OF THE THESIS

The study entitled **"DIFFERENTIAL GENE EXPRESSION ANALYSIS OF *CANDIDA ALBICANS* EXPOSED TO BIOLOGICALLY-SYNTHESIZED SILVER NANOPARTICLES"** prepared by **Osaid ALHAROUN**, and supervised by **Assoc. Prof. Dr. Hilal AY**, was found successful and unanimously accepted by committee members as Master thesis, following the examination on the date 14.8.2023.

	Title Name SURNAME **University** **Department/Art**	**Final Decision**
Chairman	Assist. Prof. Dr. Bilgin TAŞKIN Van Yüzüncü Yıl University Department of Agricultural Biotechnology	☒ Accept ☐ Reject
Member	Prof. Dr. Müberra ANDAÇ Ondokuz Mayıs University Department of Chemistry	☒ Accept ☐ Reject
Member	Assoc. Prof. Dr. Hilal AY Yıldız Technical University Department of Molecular Biology and Genetics	☒ Accept ☐ Reject

This thesis has been approved by the committee members that already stated above and determined by the Institute Executive Board.

Prof. Dr. Ahmet TABAK
Head of Institute of Graduate Studies

DECLARATION OF COMPLIANCE WITH SCIENTIFIC ETHIC

I hereby declare and undertake that I complied with scientific ethics and academic rules in all stages of my Master's Thesis, that I have referred to each quotation that I use directly or indirectly in the study and that the works I have used consist of those shown in the sources, that it was written in accordance with the institute writing guide and that the situations stated in the article 3, section 9 of the Regulation for TÜBİTAK Research and Publication Ethics Board were not violated.

Is Ethics Committee Necessary?

Yes ☐ (If it necessary, please add appendices.)

No ☒

22/06/2023
Osaid ALHAROUN

DECLARATION OF THE THESIS STUDY ORIGINALITY REPORT

Thesis Title : DIFFERENTIAL GENE EXPRESSION ANALYSIS OF *CANDIDA ALBICANS* EXPOSED TO BIOLOGICALLY-SYNTHESIZED SILVER NANOPARTICLES

As a result of the originality report taken by me from the plagiarism detection program on 22/06/2023 for the thesis titled above;

Similarity ratio : % 24

Single resource rate : % 3 has been released.

22/06/2023
Assoc.Prof. Dr. Hilal AY

ÖZET

BİYOLOJİK SENTEZLENMİŞ GÜMÜŞ NANOPARTICLES'E MARUZ KALAN *CANDIDA ALBICANS* DİFERANSİYEL GEN EKSPRESYON ANALİZİ

Osaid ALHAROUN
Ondokuz Mayıs Üniversitesi
Lisansüstü Eğitim Enstitüsü
Nanobilim ve Nanoteknoloji Ana Bilim Dalı.
Yüksek Lisans, Haziran/2023
Danışman: Doç. Dr. Hilal AY

Gümüş nanopartikülleri, terapötik özelliklerinden dolayı nanoteknoloji ve biyotıpta çeşitli amaçlar için yaygın olarak kullanılmaktadır. Bitkiler, algler, mantarlar ve bakterilerin gümüş nanopartiküllerini (AgNP'ler) biyolojik olarak üretebildiği ve bu nanopartiküllerin hücreler üzerinde antibakteriyel, antioksidan ve sitotoksik gibi çeşitli etkileri olduğu bilinmektedir. Birçok biyoaktif sekonder metaboliti üretebilen aktinobakterilerin de gümüş nanopartikülleri sentezleyebildiğine dair çalışmalar bulunmaktadır. Ancak, biyolojik olarak üretilen gümüş nanopartiküllerinin canlı hücrelere karşı gösterdiği sitotoksisitenin moleküler mekanizmaları üzerine çok az çalışma bulunmaktadır. Bu çalışmada, Antarktika'dan izole edilmiş bir aktinobakteri olan *Microbacterium* sp. H37-C3, hücre dışı olarak gümüş nanopartikülleri üretmek için kullanılmış olup biyolojik olarak sentezlenen gümüş nanopartiküllerinin *Candida albicans* üzerindeki sitotoksisitesi transkriptomik bir yaklaşımla araştırılmıştır. Biyolojik olarak sentezlenen gümüş nanopartiküllerinin fiziksel özellikleri, UV-vis spektroskopi (UV-Vis), enerji dağıtıcı X-ışını spektroskopisi (EDX) ile taramalı elektron mikroskobu (SEM) ve X-ışını kırınımı (XRD) ile karakterize edilmiştir. *Microbacterium* sp. H37-C3 tarafından sentezlenen gümüş nanoparçacıkların, 417 nm'de maksimum absorbans gösterdiği tespit edilmiştir. Gümüş nanoparçacıkların ortalama parçacık boyutu 15-30 nm arasında değişmektedir ve sentezlenen gümüş nanoparçacıklar kristal yapıdadır. Ayrıca, *Microbacterium* sp. H37-C3 suşunun tüm genom dizisi NCBI GenBank'tan indirilerek genom özellikleri ikincil metabolit biyosentetik gen kümelerini ve suşun filogenetik ilişkisini ortaya çıkarmak için analiz edilmiştir. Gümüş nanopartiküllerine maruz kalan *Candida albicans* ve kontrol grubu arasındaki diferansiyel gen ekspresyon analizi, gen ekspresyon seviyesindeki antimikrobiyal aktivite mekanizmasını ortaya çıkarmak için yapıldı. Numuneler arasında gen ekspresyon seviyelerinde istatistiksel olarak önemli bir değişiklik gözlenmemesine rağmen, gen ekspresyonunun düzenlenmesinden sorumlu olan bazı küçük nükleolar RNA'ları kodlayan genlerin ekspresyonu ile sitokrom c oksidaz ve telomer uzunluğunun korunmasından sorumlu bazı genlerin ekspresyonu AgNP işleminden etkilenmiştir. Sonuçlar, gümüş nanopartiküllerin ökaryotik hücreler üzerindeki toksisite mekanizmalarının gen ekspresyon seviyesinde anlaşılmasına katkı sunmaktadır.

Anahtar Sözcükler: Aktinobakteriler, Biyojenik gümüş nanopartikülleri, *Candida albicans*, RNA-dizileme, Transkriptomik

ABSTRACT

DIFFERENTIAL GENE EXPRESSION ANALYSIS OF *CANDIDA ALBICANS* EXPOSED TO BIOLOGICALLY-SYNTHESIZED SILVER NANOPARTICLES

Osaid ALHAROUN
Ondokuz Mayıs University
Institute of Graduate Studies
Department of Nanoscience and Nanotechnology
Master, June/2023
Supervisor: Assoc. Prof. Dr. Hilal AY

Silver nanoparticles are extensively used in nanotechnology and biomedicine for various purposes due to their intrinsic therapeutic properties. Plants, algae, fungi, and bacteria have been known to produce silver nanoparticles (AgNPs) biologically, and those nanoparticles have various effects on the cells, such as antibacterial, antioxidant, and cytotoxic. There are reports showing that actinobacteria producing many bioactive secondary metabolites could produce silver nanoparticles. In this study, an actinobacterium isolated from Antarctica, *Microbacterium* sp. H37-C3 was used to produce silver nanoparticles extracellularly, and the cytotoxicity of these biologically synthesized silver nanoparticles on *Candida albicans* was investigated by a transcriptomic approach. The physical properties of the synthesized silver nanoparticles were characterized by UV–visible spectroscopy (UV–Vis), scanning electron microscopy (SEM) with energy-dispersive X-ray spectroscopy (EDX), and X-ray diffraction (XRD). It was determined that the silver nanoparticles synthesized by Microbacterium sp. H37-C3 showed the maximum absorbance peak at 417 nm. The average particle size of the silver nanoparticles ranges from 15-30 nm, and the synthesized silver nanoparticles are in crystalline structure. Moreover, genome characteristics of strain *Microbacterium* sp. H37-C3 was also analyzed to reveal secondary metabolite biosynthetic gene clusters and the phylogenetic relationship of the strain by downloading the whole-genome sequence of the strain from the NCBI GenBank database. Differential gene expression analysis between silver nanoparticle-exposed *Candida albicans* and the control group was conducted to reveal its antimicrobial activity mechanism in gene expression level. Although no statistically significant change in the gene expression levels was observed between the samples, the expression of several genes coding for small nucleolar RNAs as well as the expression of the gene coding for cytochrome c oxidase and a gene responsible for maintenance of telomere length was affected by the AgNP treatment. The results contribute insight into the toxicity mechanisms of silver nanoparticles on eukaryotic cells at the gene expression level.

Keywords: Actinobacteria, Biologically-synthesized silver nanoparticles, *Candida albicans*, RNA-sequencing, Transcriptomics.

ACKNOWLEDGEMENT

I want to start by thanking Dr. Hilal Ay, my research supervisor. I want to take this opportunity to thank her from the bottom of my heart for helping me to conduct my research and for the vital guidance I received while conducting it. Working and studying with her was a real honor and privilege.

In addition, I want to thank everyone who supported me while working at Ondokuz Mays University's Department of Nanoscience and Nanotechnology.

My sincere appreciation to my family, especially my mother and father, for the endless affection and sacrifices that helped me grow up and prepare for the future. Without them, I would not have arrived at this moment.

Osaid ALHAROUN

CONTENTS

SYMBOLS AND ABBREVIATIONS

Ag-NPs	: Silver nanoparticles
NPs	: Nanoparticles
Nm	: Nanometer
EDS	: Energy-Dispersive Spectroscopy
SEM	: Scanning Electron Microscopy
XRD	: X-Ray Diffraction
DLS	: Dynamic light scattering
TEM	: Transmission electronic microscopy
AFM	: Atomic Force Microscopy
UV -VIS	: Ultraviolet-Visible Spectroscopy
MIC	: Minimum Inhibitory Concentration
FTIR	: Fourier Transform Infra-Red
NGS	: Next-generation sequencing
DGG	: Differential gene expression
G+C	: guanine and cytosine
snoRNA	: Small nucleolar RNA
TPM	: transcripts per million
FPKM	: Fragments Per Kilobase of transcript per Million
CA	: Control sample
CA-Nano	: Treated sample (AgNP-exposed)
PCR	: Polymerase chain reaction
qPCR	: Quantitative real-time PCR
Ag2O	: Silver oxide
RPM	: Revolutions per minute

FIGURES LEGENDS

TABLES LEGENDS

1. INTRODUCTION

It is no lo nger hidden from anyone the spread and expansion of fungi resistant to the available antifungal drugs. Moreover, antifungal drugs, especially systemic ones, have many side effects, some of which cannot be ignored, such as nephrotoxicity and ototoxicity. *Candida albicans*, which is an opportunistic fungus, is the cause for a wide range of superficial and systemic fungous infections, making it one of the most prevalent types of fungi. It usually only causes disease in individuals whose immune system is compromised or whose natural flora is altered.

Fungi, much like their human hosts, are eukaryotes. So, there aren't many distinctive biochemical targets that can be used to generate new antifungal drugs. Only three primary types of medications are now approved in order to treat invasive fungous infections, and the development of drug resistance in pathogen populations compromises the effectiveness of these medications (Yunjin Lee et al., 2021).

The most prevalent yeast isolate in blood infections is *Candida albicans*. *Candida albicans* is the predominant species of *Candida* responsible for causing candidemia, a situation attributed to the presence of *Candida* in the bloodstream, which remains a highly prevalent and life-threatening condition, leading to substantial morbidity and mortality according to a retrospective study conducted from 2011 to 2017 (Xiao, Z et al., 2019).

Approximately 7% of *Candida* blood specimens examined at the Centers for Disease Control and Prevention (CDC) exhibit resistance to the antimycotic medication fluconazole (Toda M et al., 2019).

As a result of the aforementioned reasons, attempts have begun to seek new medicines that have fewer side effects on the one hand and are more capable of overcoming resistance on the other. Among the most important and latest research in this field, nanoparticles had a large share. The surface-to-volume ratio of nano-sized metal particles is a distinctive characteristic, which dramatically alters physical, chemical, and biological properties. among the most distinctive types of nanoparticles were silver nanoparticles (AgNPs). Due to their distinct physical and chemical features, they exhibit bactericidal, fungicidal, and virucidal properties.

To meet the requirements of AgNPs, various synthetic methods have been

employed. Traditional physical and chemical techniques generally seem to be exceedingly costly as well as hazardous. Interestingly, The bio-fabricated AgNPs exhibited notable attributes such as stability, solubility, and high productivity. Among various methods available for synthesizing AgNPs, biological approaches appear to be the most practical, efficient, secure, dependable, and ecologically harmless.

Several studies have found size and shape of silver nanoparticles have a significant role in their antimicrobial efficacy. Therefore, we must mention here that the size and shape of the silver nanoparticles may change depending on the type of micro-organisms used in the synthesis.

Table 1.1 presents the observed alterations in the shape and size of silver nanoparticles, which were synthesized using various microorganisms.

Table 1.1. Synthesis of AgNPs using some kinds of bacteria and fungus

Silver Salt	**Microorganisms**	**Shape**	**Silver Size (nm)**	**Reference**
AgNO3	*Bacillus licheniformis*	Spherical	18–63	(Abdel-Hafez et al., 2016)
AgNO3	*Gluconacetobacter xylinus*	Spherical	40–100	(Du et al., 2018)
AgNO3	*Bacillus pumilus*	Spherical	77–92	(El-Bendary et al., 2020)
AgNO3	*Phanerochaete chrysophobia*	Pyramidal	50–200	(Huang et al., 2020)
AgNO3	*Fusarium oxysporum*	Spherical	5–15	(Dutta et al., 2020)

Differential gene expression analysis is a powerful tool that allows for a deeper comprehension of the mechanisms behind the effects of nanoparticles on microorganisms. In our research, we studied the impacts of bio-synthesized AgNPs on the gene expression profile of *C. albicans* using RNA sequencing technology. Specifically, we aimed to determine genes that are expressed differently and signalling pathways that go into the response of *C. albicans* to silver nanoparticles that were prepared by strain H37-C3.

2. LITERATURE REVIEW

2.1. Synthesis of silver nanoparticles

Silver nanoparticles (AgNPs) can be created using a variety of techniques, including physical, chemical, and biological ones.

1-Physical methods: like laser ablation, vaporization & condensation methods, and ball milling, are used produce AgNPs (Yaqoob et al., 2020).

2-Chemical methods: In chemical methods, the size, shape, and surface characteristics of the nanoparticles are controlled through the use of reducing agents, stabilizers, and surfactants. These methods are relatively simple and have a high yield. There are many disadvantages when utilizing reducing agents, including their toxicity, weak reducing capacity, and contaminants. (Jamkhande et al., 2019).

3-Biological methods: To produce AgNPs, biological techniques use organisms like fungi, bacteria, and plants. These procedures are low-toxic, economical, and environmentally friendly (Jamkhande et al., 2019).

2.2. Actinomycetes

The phylum *Actinomycetota* which is recognized as one of the most important taxonomic groups within the bacterial world consists of microorganisms known as actinomycetes (De Simeis and Serra, 2021).

Gram-positive microorganisms come from the *Actinomycetota* phylum typically possess a high DNA guanine-cytosine (G + C) content. This content varies among different species, with certain corynebacteria exhibiting a G + C content of around 51%, while *Streptomyces* and *Frankia*, among others, can have G + C content exceeding 70% (Ventura et al., 2007).

2.2.1. Synthesis of NPs by Actinomycetes

Actinomycetes, a group of bacteria within the phylum *Actinomycetota*, are considered valuable sources for the synthesis of nanoparticles (NPs). They possess a diverse range of secreted secondary metabolites, which contribute to the production of NPs with desirable surface and size characteristics. Actinobacteria have the potential of producing metallic NPs both intracellularly and extracellularly. Extracellular synthesis of NPs by actinomycetes has gained additional commercial

advantages compared to intracellular synthesis due to the role of polydispersity. The extracellular approach allows for the production of NPs with a wider range of sizes and shapes, leading to a more diverse and potentially useful nanoparticle population. This polydispersity can be advantageous for various applications where a mixture of NPs with different properties is desired (Manivasagan et al., 2014)

Actinomycetes possess an unparalleled ability to produce a variety of secondary metabolites, particularly antibiotics and anti-toxins (Salem and Gobouri, 2020).

Bacterial cells will be exposed to AgNO3 throughout the intracellular production process and cultured under the proper growth conditions. To prevent the presence of medium components during the interaction, microorganisms need to be rinsed by sterile distilled water beforehand (Wypij et al., 2018).

In the interaction process, silver ions are captured on the surface of the cell as a result of the electrostatic attraction between the silver ions and the negatively charged cell wall. Subsequently, reduction processes facilitated by proteins, enzymes, or other factors take place, resulting in the production of silver nanoparticles behind the cell wall (Lee and Lee, 2019).

In a similar manner, actinobacterial cell-free extract, which contains proteins, enzymes, and other bioactive compounds, exhibits the ability to create silver nanoparticles when treated with $AgNO_3$. The cell-free extract functions as both a reducing agent, facilitating the conversion of Ag+ ions to silver nanoparticles, and a stabilizing agent, preventing their aggregation and maintaining their stability (Dong et al., 2017).

2.2.2. The Genus *Microbacterium*

The *Microbacterium* genus is classified within the *Microbacteriaceae* family, which is a taxonomic group of actinobacteria known for its high G+C content. It differs from other actinomycetes in the combination of abnormal B-group peptidoglycans in the cell wall and unsaturated respiratory menaquinones. With over 90 recognized species, the genus *Microbacterium* has been isolated from various habitats and hosts, showcasing its wide ecological distribution (Hadjadj et al., 2016).

In this study, an actinobacterium, *Microbacterium* sp. H37-C3, isolated from a rock sample collected on Horseshoe Island (Antarctica), was used to produce silver nanoparticles extracellularly. This shows a 98.47% similarity in its 16S rRNA sequence with *Microbacterium arborescence*. *Microbacterium arborescence* is an aerobic, Gram-positive, rod-shaped bacterium that produces yellow-colored colonies. They are rarely isolated from the environment. No human infections have been reported. Strain H37-C3 is representative of a novel species within the genus *Microbacterium*. Given that novel actinobacteria may synthesize unique metabolites, the silver nanoparticles synthesized by novel strains may also have considerable bioactivity and biotechnological potential for the pharmaceutical industry.

2.3. Candida *albicans* as a Pathogen and Pathogenicity Mechanisms

As we mentioned *Candida albicans* is a common commensal fungus but for many reasons, it turns into a pathogenic form. Though some of these factors are caused by changes related to the host such as immunosuppression, other factors result from changes at the genetic level of *Candida albicans*, which increase its virulence and resistance to the immune system and antifungals. virulence factors such as the synthesis of tissue-damaging enzymes, hyphal morphogenesis, and biofilm development.

Candida albicans have various morphological forms which include blastospores, pseudohyphae, and hyphae. going from yeast to hyphal form represents a transition into a pathogenic state (Mayer et al., 2013).

Mutants that are incapable of forming hyphae under *in vitro* conditions generally exhibit reduced virulence (Lo et al., 1997).

Various factors, including genes (such as adhesins) and gene products (such as secreted enzymes), perform a significant role in the virulence of bacteria. These virulence factors contribute to the interaction between the bacterium and the host, leading to the development of both superficial and invasive infections in humans (Casadevall, 2007).

Some of the most important genes that related virulence of *Candida albicans* are for instance SAP5 (secreted aspartyl proteases) and ECE1 which have an essential role in penetrating deeper tissues and interacting with host defences during infection. The expression of SAP5 is significantly increased in biofilms cultivated *in*

vivo and in a reconstituted human epithelium (RHE) model of infection (Nailis et al., 2010).

The ECE1 gene encodes candidalysin, that is believed to be attributed to essential virulence features of *Candida albicans* such as adhesion, biofilm formation, and filamentation capabilities (Satiman et al., 2020)

Also, we cannot ignore ALES genes, which have a great role in virulence. Als3 mediates adhesion to various host substrates. To colonize mucosal surfaces and initiate disease, *Candida albicans* must adhere to host components. The ALS3 gene, which is specifically expressed by *C. albicans* hyphae and pseudohyphae, plays a crucial role in this attachment process. It is worth noting that ALS3 is not expressed in yeast-phase organisms of *C. albicans* (Argimón et al., 2007).

Also, one of the important genes that should be mentioned is the gene encoding for hyphal wall protein (Hwp1) which it's important emerged for the pathogenesis of candidiasis. "Biofilm and Cell Wall Regulator 1" (Bcr1) is a transcription factor necessary for the development of biofilms and is expressed more abundantly in hyphae, suggesting that hyphal components produced by Bcr1-dependent genes may be necessary for the development of biofilms (Nobile and Mitchell, 2005).

2.3.1. Drug Resistance Mechanisms in *Candida Albicans*

In the last years, we witnessed the aspect where current antifungal effectiveness is diminishing over time and not able to overcome fungus disease. Therefore, in order to overcome this resistance and develop novel therapeutics, it was necessary to understand the mechanisms and algorithms developed by these organisms to become resistant to traditional antifungals.

The primary categories of current antifungal drugs and the mechanisms underlying drug resistance are as follows:

- Polyenes, which are natural amphiphiles, were among the first family of antifungal medications employed to treat widespread fungal infections. The major sterol presents in fungal cell membranes, ergosterol, serves as a binding site for these medications. The binding results in depolarization of the membrane, which in turn raise its permeability. This enhanced permeability leads to the leakage of

intracellular cations, ultimately causing cell death. Polyene antifungals include drugs like nystatin and amphotericin B (Haro-Reyes et al., 2022).

Resistance to polyenes, such as amphotericin B, has been associated with alterations in the ERG3 and ERG6 genes. In laboratory studies, the disruption of ERG3 and ERG6 has been observed to result in decreased levels of ergosterol, the target molecule of polyene drugs. This reduction in ergosterol levels has been linked to higher resistance to amphotericin B in *Candida albicans* and *Candida glabrata*. However, little is known about polyene resistance in clinical isolates (Vandeputte et al., 2012).

- Azoles are widely used as antifungal agents as a result to their broad-spectrum activity, chemical stability, and oral bioavailability. The azoles of antifungal agents are divided into two subclasses: imidazoles and triazoles. It is generally believed that they inhibit cytochrome P450-dependent enzymes involved in cell membrane sterol biosynthesis as well as induce the formation of toxic byproducts that are lethal to fungi. Examples of imidazoles are clotrimazole, miconazole, and ketoconazole while fluconazole, itraconazole are a good example of triazoles (Shafiei et al., 2020).

There are numerous ways in which *Candida albicans* could develop resistant to azoles, such as:

1-*Candida albicans* can become resistant to azoles by increasing the number of efflux pumps in the wall of microorganism cell. Two gene groups of transporters—the multiple drug resistance (MDR) genes of the major facilitators class (MFS-transporters) and the CDR genes contributing to the ATP-binding domain family (ABC-transporters)—encode efflux pumps in *Candida* species (Albertson et al., 1996); Sanglard et al., 1997).

For example, azole-resistant clinical isolates of *Candida albicans*, whether found in oral, *systemic*, or vaginal infections, often exhibit a common phenomenon: the excessively expression of particular efflux pump genes, namely CaCDR1, CaCDR2, and CaMDR1 (Bhattacharya et al., 2016)

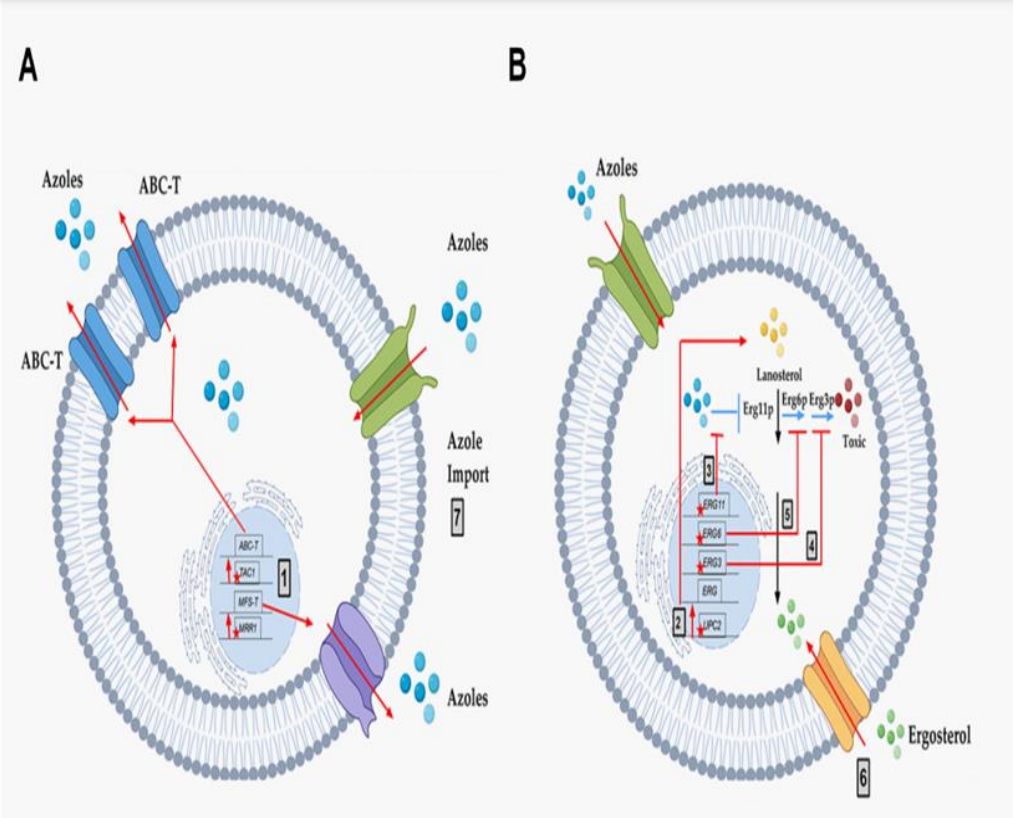

Figure 2.1. The molecular mechanisms of azole resistance.

The provided diagram illustrates the mechanisms that contribute to azole resistance in pathogenic fungi. black arrows show the regular ergosterol route The green circles represent ergosterol, which has an inhibitory effect on UPC2 whereas the yellow circles represent lanosterol. The blue arrows show the azole drug's mechanism of action, that includes suppressing the target Erg11p and producing toxic diol through a series of stages, including Erg6p and Erg3p (red circles).

The chromosomal positions of the resistance-related genes are indicated by black rectangles inside the nucleus. Red stars show mutations that result in resistance, whereas red arrows show the associated molecular paths. The following is an explanation of the azole resistance pathways in pathogenic fungi:

(A) The efflux pump activity-based azole resistance mechanism is shown in grey box 1. mutations in MRR1 and TAC1 (stars) promote overexpression of MFS-Ts and ABC-Ts, respectively. As a consequence, azole efflux is amplified.

(B) The synthesis of ergosterol is changed as part of the azole resistance mechanism, indicated in grey boxes 2, 3, 4, 5, 6, and 7. These involve point

mutations in UPC2 (grey box 2), resulting in increased expression throughout the ergosterol pathway; mutations in ERG11 (grey box 3), preventing azole binding; mutations in ERG3 (grey box 4), preventing the formation of toxic sterol; mutations in ERG6 (grey box 5), preventing the formation of toxic sterol; sterol import (grey box 6), decreasing the demand for sterol synthesis and changing the flow of azoles (grey box 7), reducing intracellular azoles (Bhattacharya et al., 2020).

2- Overexpressed or mutated ergosterol biosynthesis genes

ERG11/CYP51Erg11p, a cytochrome P450 enzyme, performs an essential function in the control of a rate-limiting step in the pathway that synthesis ergosterol (Veen et al., 2003).

Increased expression of CaERG11 is frequently seen in clinical specimens of C. albicans that have become more resistant to azole drugs (Bhattacharya et al., 2016).

A single mutation in the ERG11 gene, which encodes for lanosterol 14α-demethylase, can result in totaly loss of binding ability of the azole drugs to its intended target (Marichal et al., 1999).

-Allylamines which affect the synthesis of ergosterol through inhibition of the enzyme squalene epoxidase and as a result increase the transformation of squalene to squalene epoxide. Squalene epoxide is toxic to the fungal cell. terbinafine and naftifine are examples of allylamines (Ahmed et al., 2021).

- Echinocandins are a group of antifungal medications that target the cell wall. Examples of echinocandins include caspofungin, micafungin, and anidulafungin. These drugs work by targeting the enzyme β1-3 glucan synthase, which is coded by the FKS1, FKS2, and FKS3 genes (Perlin, 2011).

Resistance of *C. albicans* to echinocandin drugs primarily occurs through target site alteration. This involves the presence of point mutations in either the FKS1 or FKS2 genes, which are responsible for encoding the target enzyme affected by echinocandins (Balashov et al., 2006).

2.4. RNA Sequencing

The analysis of data regarding genome-wide mRNA expression has been made

easier by next-generation sequencing technology. Gene expression levels indicate the variation between samples through analysis of RNA-sequencing data. Comprehension of transcriptome-wide alterations in many model systems. To get the required outcomes, it has been highly helpful to develop open-access software tools for conducting differential expression (DE) analysis. The majority of RNA-seq experiments use pure RNA samples that are converted to cDNA and then sequenced using high-throughput platforms like SOLiD, Illumina GA/HiSeq, and Roche 454 in a The process that generates millions of short reads (between 25 and 300 bp) (Shendure and Ji, 2008)

The following step within this procedure is read alignment, which seeks to determine where each short read most closely matches the reference. Then we should summarize the mapped reads, we can go through this process to calculate the mapped reads for genomic features, such as exons, transcripts, or genes. The RNA-Seq study then moves on to normalization, which modifies the raw data to take into account variables that influence comparisons of expression levels. like length, GC content, and sequencing depth. Then we get to the last step Differential Gene Expression (DE) analysis, through which we can determine which genes are up- or down-regulated as a result of exposure to an external factor.

RNA-Seq provides several advantages, including:

- With RNA-Seq, identified and new transcripts may be reassembled at the single-base level.

- The dynamical spectrum of RNA-Seq is wide and is not constrained by signal saturation..

-RNA-Seq data exhibit high levels of reliability.

2.5. RNA-seq and Differential Gene Expression Analysis

Microorganism's DNA contains all the information required for each cell's characteristics and functions. Through the process of gene expression, cells can selectively activate and deactivate specific genes, allowing them to access and translate specific instructions. The information contained within these selected genes is transcribed into RNA strands, which are either utilized by the cell directly or translated to other molecules. Therefore, the collection of transcribed RNAs in a

given condition provides insight into the situation of a cell currently and may reveal the underlying response pathwayes in different conditions.

The RNA-seq sequencing framework enables the comprehensive analysis of all RNA molecules within a sample at a detailed level. It involves characterizing their sequences and simultaneously determining their abundance. actually, millions of random reads are obtained from RNA sample, which can then be mapped to a reference genome employing computational approaches. This alignment process generates a "transcriptome map" where the amount of reads mapped indicate the level of expression for each gene. Numerous computational applications have been designed and continually upgraded to support this process, reflecting the rapid growth in this field. One of RNA-seq's greatest attributes is that it's able to provide single-base resolution, which enables accurate quantification and sequencing of all the specimen's transcripts.

The two basic subcategories of differential gene expression analysis techniques in RNA-Seq are parametric and non-parametric. Parametric strategies utilize the parameters to involve all available information about the data. By applying a specific model and its parameters, the values of unknowable data can be predicted. When parametric strategies are employed for differential gene expression analysis, a normalization step is often performed, where each gene's expression value is matched to a certain distribution, such as the Poisson distribution or the negative binomial distribution. Non-parametric approaches, on the contrary, incorporate more thorough information about the data distribution without applying a strict model that needs to be adapted. Non-parametric models assume that a finite number of parameters cannot properly describe the data distribution. Therefore, as the volume of data increases, non-parametric strategies are capable of incorporating a larger amount of information about the data distribution (Costa-Silva et al., 2023).

There are numerous tools available for RNA-Seq differential expression analysis. Examples include the negative binomial model as the primary approach in DESeq2, edgeR, and baySeq, among others. On the other side, non-parametric approaches are used by alternative software tools like NOIseq and SAMseq. Currently, there is no unanimity regarding the most suitable approach that guarantees the integrity, accuracy, and reliability of the results. This field in Bioinformatics is

still growing.

Rather than just employing normalization to fix data, DESeq2 also uses its own library inconsistencies. Additionally, the input data for DESeq2 must be in the form of an integer matrix. while EdgeR and limma utilize normalized RNA-Seq count data (Liu et al., 2021).

baySeq: By using the Bayesian empirical technique, baySeq can identify the differential expression patterns for each gene by estimating the posterior probability of each set of models (Hardcastle and Kelly, 2010).

DESeq: Using a negative binomial distribution with local regression to limit the variance and mean (love et al., 2014).

edgeR: To take into account both technical and biological variations, edgeR uses a Poisson super dispersion model. The level of transcript over-dispersion is regulated using the Bayesian empirical approach (Robinson et al., 2009).

limma+voom: Originally created for analyzing data from microarrays, the linear model has been adapted for RNA-Seq analysis. The limma user guide suggests utilizing the TMM normalization method supplied by the edgeR package. This normalization process converts the normalized counts into logarithms with a base of 2, and it measures the mean and variance for each initial observation using a linear model (Law et al., 2014).

NOIseq: It empirically models the noise contained in the counting data and is non-parametric enabling data analysis even without duplicates. (Tarazona et al., 2011).

SAMseq: For sequencing counts with various depths, a non-parametric technique with resampling is used. It may be used with two-class, multiple-class, or data with quantitative outcomes (Tarazona et al., 2015).

DESeq2: In the beginning, DESeq2 creates a model by employing obtained counts. Second, it works when applying the original DESeq approach., as an alternative it fits in a pair of steps as follows: This process, known as maximum likelihood estimation, involves finding the parameter value that maximizes the likelihood. Then, it averages the gene values by taking into account all of the values for each gene. For determining how much movement should be made for each gene,

DESeq2 follows the Bayes theorem: if the gene's information is low, its value is moved approximately in line with the average, and if the gene's information is high, very little movement is made. In order to apply a threshold and analyze several groups of genes, it is helpful to utilize the moved values (Love et al., 2014).

2.6. Algorithms For The Alignment Process

As previously stated, the initial process for RNA-seq data analysis involves read alignment, for which various alignment tools were developedThe mapping process always starts by creating an index of the reference genome or the readings., depending on the specific situation. This index is then utilized to efficiently retrieve the regions within the reference sequence where read alignment is most likely to take place. The process of alignment is carried out after a list of appropriate mapping positions has been observed using slower and more sensitive algorithms within these candidate regions (Hatem et al., 2013).

Despite all these noteworthy details and what appear to be simple data, RNA-seq investigations result in vast and complicated amounts of data that are difficult to analyze (Oshlack et al., 2010).

Technical difficulties peculiar to the NGS technique, such as sequencing mistakes in the output reads caused by incorrectly called bases, make data processing even more difficult (Shendure and Ji, 2008).

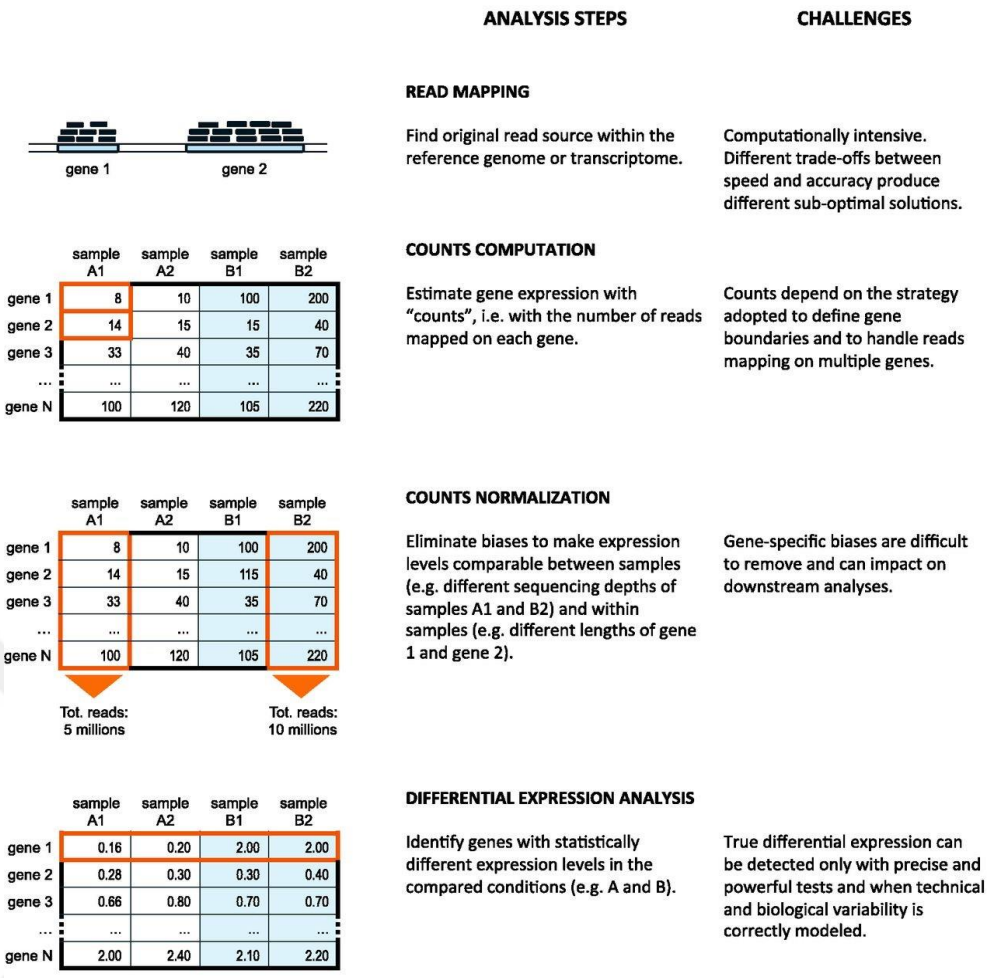

Figure 2.2. The primary technical obstacles and computational procedures for DE analysis of RNA-seq data (Finotello and Di Camillo, 2014).

2.7. Factors Affecting NPs Synthesis

Several factors influence the biosynthesis of nanoparticles (NPs). These factors can be attributed to changes in the surrounding environment or the presence of bioactive agents. For successful NP synthesis, the reaction mixture must have the ideal metal ion concentration, temperature, and pH degrees. Furthermore, technical factors like the pH, concentration of the substrate, temperature, and exposure period to the substrate might influence the degree of intracellular NP synthesis and the size of the NPs (Verma and Mehata, 2016).

3. MATERIALS AND METHODS

3.1. Green Synthesis of Silver Nanoparticles

Silver nanoparticles were synthesized by *Microbacterium* sp. H37-C3, which was isolated from Horseshoe Island (Antarctica) in the scope of another project performed in the 6th Turkish Antarctic Expedition. The cells of *Microbacterium* sp. H37-C3 were activated in tryptone- yeast- extract- glucose- agar (TYG) (tryptone 3 g/l, yeast extract 5 g/l, glucose 5 g/l, agar 15 g/l, distilled water 1000 ml, pH 7.0) and glucose-yeast extract-malt extract agar (GYM) (glucose 4 g/l, yeast extract 4 g/l, malt extract 10 g/l, agar 20 g/l, distilled water 1000 ml, pH 7.2).

Following growth on agar media, colonies of the strain were carefully selected and transferred into 30 ml of sterile Tryptic Soy Broth (TSB) with a pH of 7.0. The culture was then incubated at 20°C on a closed rotary shaker, set at 150 rpm, for a duration of 3 days. Afterward, 5 ml of the culture was transferred into a flask containing 100 ml of sterile TSB. The flask was again placed on a closed rotary shaker at 20°C and 150 rpm, this time for 4 days. Upon completion of the incubation period, the broth was subjected to centrifugation at 8000 rpm for 20 minutes at 4°C. The resulting supernatant was collected and mixed with a solution of 2 mM $AgNO_3$ (v/v). The mixture was then incubated on a closed rotary shaker at 150 rpm for 7 days, maintaining a temperature of 50°C in dark conditions. The resulting silver nanoparticles were then washed with distilled sterile water to remove any residual impurities. The particles were then dried at 55°C by a dry block heater.

3.2. Characterization of Silver Nanoparticles Synthesized by *Microbacterium* sp. H37-C3

The synthesized silver nanoparticles underwent characterization using various analytical techniques, including UV-vis spectroscopy, SEM-EDX and XRD. UV-Vis spectroscopy was employed to measure the absorption and scattering of light by the nanoparticles. UV-Vis spectra provide information about the surface plasmon resonance (SPR) of the nanoparticles, which is indicative of their size and shape. XRD analysis was used to determine the crystal structure and composition of the synthesized nanoparticles. By measuring the scattering of X-rays, it can provide information about the arrangement of atoms in the nanoparticles and their crystalline

nature. Scanning electron microscopy (SEM) was used to visualize the nanoparticle morphology and size distribution. It provides high-resolution images of the nanoparticles and can reveal their shape, surface features, and agglomeration behavior. In addition, energy-dispersive X-ray spectroscopy (EDX) analysis was performed alongside the SEM analysis and to get information about the elemental composition of the nanoparticles. It identifies the presence and relative abundance of different elements within the nanoparticles.

3.3. Genome Analysis of *Microbacterium* sp. H37-C3

The genome sequence data of *Microbacterium* sp. H37-C3 was downloaded from the GenBank database NCBI by the accession number. For the taxonomic analysis the sequence of Microbacterium sp. H37-C3 was uploaded to the Type Strain Genome Server (TYGS) https://tygs.dsmz.de (Meier-Kolthoff and Göker, 2019).

The secondary metabolite coding gene clusters of *Microbacterium* sp. H37-C3 was determined by uploading the genome sequence to antibiotics and a secondary metabolite analysis server (antiSMASH) available at https://antismash.secondarymetabolites.org/#!/start (Blin et al., 2023).

3.4. Inhibitory Activity of Silver Nanoparticles Synthesized by *Microbacterium* sp. H37-C3 against *Candida albicans*

The *Candida albicans* culture was activated in Mueller Hinton agar (MHA), using a sterilized wire-loop and transferred to the agar in a petri-dish then spread all over the surface carefully in a linear pattern, followed by the incubation at 37°C for 24-48 hours. The minimum inhibition concentration (MIC) of the synthesized silver nanoparticles against *C. albicans* was determined by modifying the agar dilution method (Wiegand et al., 2008). The activated *C. albicans* culture was suspended in sterile Ringer's solution (Oxoid) to obtain an optical density between 0.5-1.0 corresponding to 1.5-3.0 x 108 CFU/ml. A volume of 200 µl pathogen suspension was spread onto MHA medium. At the same time, a silver nanoparticle solution of 1 mg/ml was diluted to obtain 0.5 mg/ml, 0.25 mg/ml, and 0.125 mg/ml solutions. A volume of 200 µl of the diluted silver nanoparticle solutions was spread onto the pathogen-inoculated MHA plates. The inoculated plates were incubated at 37°C for 48 h.

3.5. Exposure of *Candida albicans* with Silver Nanoparticles

After determining MIC against *C. albicans*, MIC_{10} was used for the exposure experiment. Nutrient broth medium including AgNPs at MIC_{10} concentration was inoculated with *C. albicans* strain suspended in Ringer's solution at McFarland 4.0 density. The culture medium without AgNPs was prepared as the control. After 17 h incubation at 37°C in a shaker incubator (100 rpm), the cultures were centrifuged at 4°C at 8000 rpm for 10 min and suspended in glycerol solution (40%, v/v).

3.6. RNA-Seq Analysis

RNA sequencing for the AgNP-exposed *C. albicans* and control group was performed by Macrogen Inc. (Korea). Firstly, the RNA extraction was performed and the samples that pass quality assurance requirements moved on to the library development process. The library preparation was performed by NEBNext rRNA Depletion (Bacteria) and TruSeq Stranded Total RNA Library Prep Gold Kit. Briefly, the random fragmentation of the cDNA samples, followed by the ligation of the 5' and 3' adapter, were used to generate the sequencing library. With a PCR primer solution that anneals to the ends of each adapter, fragments that had been adapter-ligated were then amplified. The library templates underwent quality control and quantification process. The library was placed onto a flow cell, where fragments were collected on a lawn of surface-bound oligos that complemented the library adapters. Then, using bridge amplification, each fragment was amplified into a unique clonal cluster. The templates were prepared for sequencing on an Illumina platform once cluster creation was finished. Raw pictures were produced by the Illumina sequencer using integrated primary analysis software called RTA (Real Time Analysis), which also served as the system control and base calling software. The BCL/cBCL (base call) binary files were converted into FASTQ files using bcl2fastq provided by the Illumina. The overall experimental workflow was summarized in Figure 3.1

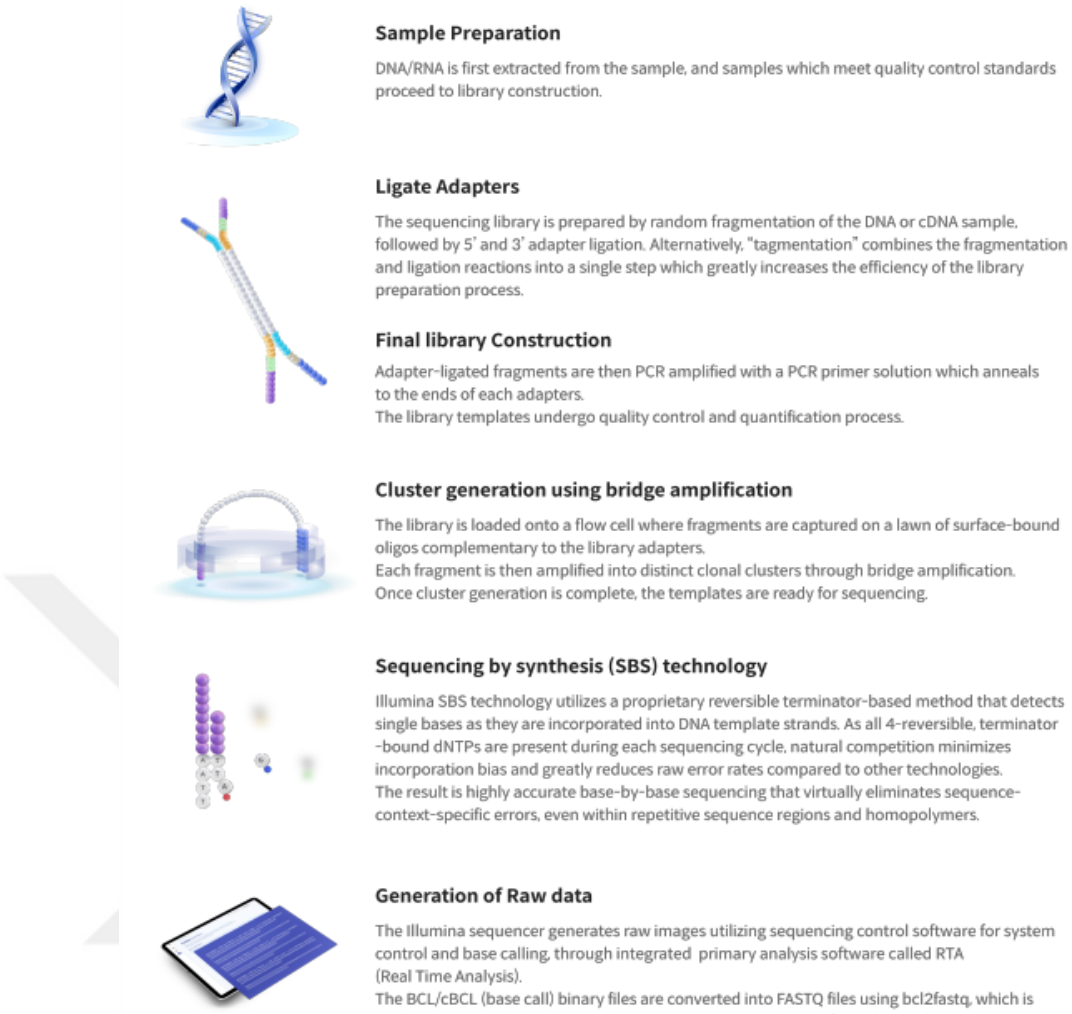

Figure 3.1. The experimental workflow for RNA sequencing on an Illumina platform (Macrogen Inc.)

The differential gene expression analysis was performed on KBase server (Arkin et al., 2018) available at https://www.kbase.us/. Firstly, an RNA-Seq sample set including the raw reads for the CA (control) and CA-Nano (AgNP-exposed group) samples was constructed on the KBase server. The quality control of the reads was performed by FastQC - v0.12.1 algorithm (http://www.bioinformatics.babraham.ac.uk/projects/fastqc/). The low-quality reads and adapter sequences were removed by Trimmomatic - v0.36 (Bolger et al., 2014). The alignment of the trimmed reads against the reference genome of *C. albicans* available at the KBase server was acquired by using TopHat2 v1.0.1 (Kim et al.,

2013). The aligned transcripts were assembled using Cufflinks v2.2.1 algorithm (Trapnell et al., 2010). The differential gene expression analysis was performed by using Cuffdiff v2.2.1 (Trapnell et al., 2010) available at the KBase platform.

4. RESULTS AND DISCUSSION

4.1. Synthesis of Silver Nanoparticles

The green synthesis of silver nanoparticles was acquired by the culture supernatant of *Microbacterium* sp. H37-C3 (Figure 4.1).

Figure 4.1. The growth of *Microbacterium* sp. H37-C3 on GYM medium agar

During the incubation period, a noticeable change in color occurred, with the solution turning into a dark reddish-brown shade. This change refers the successful formation of silver nanoparticles (AgNPs) within the culture solution. It is worth noting that silver nanoparticles typically exhibit a brown color in aqueous solutions due to the surface plasmon resonance effect. To separate the silver nanoparticles from the solution, microcentrifugation was performed at 14000 rpm for 20 minutes.

(a) (b)

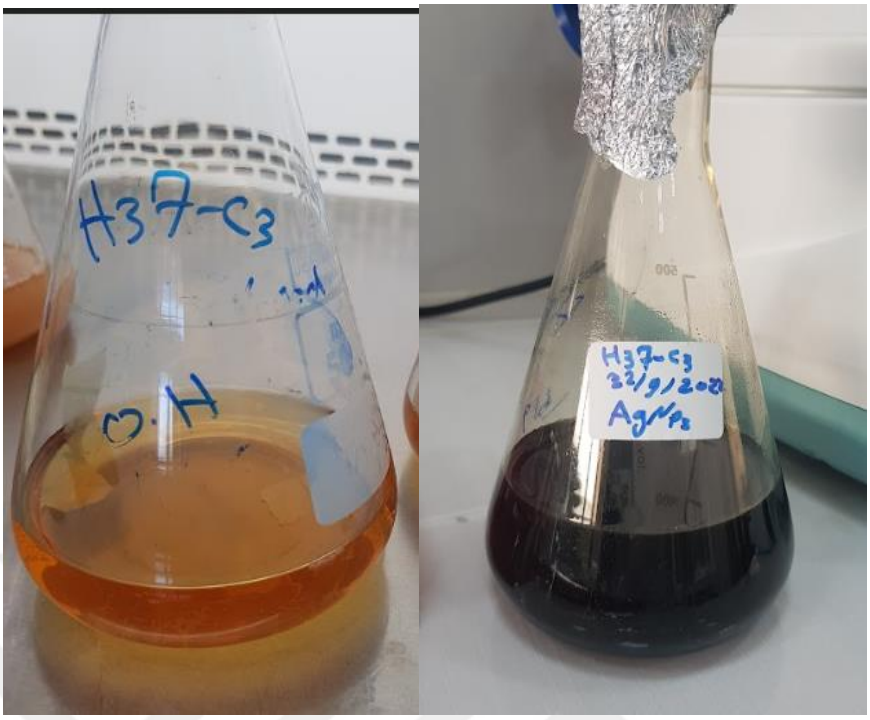

Figure 4.2. Silver nanoparticle cultivation is indicated by a change in color (a) supernatant without AgNO3 (b) formation of AgNPs

4.2. Physicochemical Characterization of the Silver Nanoparticles

The initial characterization of the silver nanoparticles (AgNPs) was conducted using UV-Visible spectroscopy. The absorbance spectra of the AgNPs solution were recorded using a UV-Vis spectrophotometer over a wavelength range of 200 to 790 nm. It is well-known that AgNPs exhibit a characteristic absorption peak in the UV-Visible region, typically ranging from 400 to 500 nm, which corresponds to the phenomenon of surface plasmon resonance (Sastry et al., 1997). The silver nanoparticles synthesized by *Microbacterium* sp. H37-C3 showed the maximum absorbance peak at 417 nm (Figure 4.3).

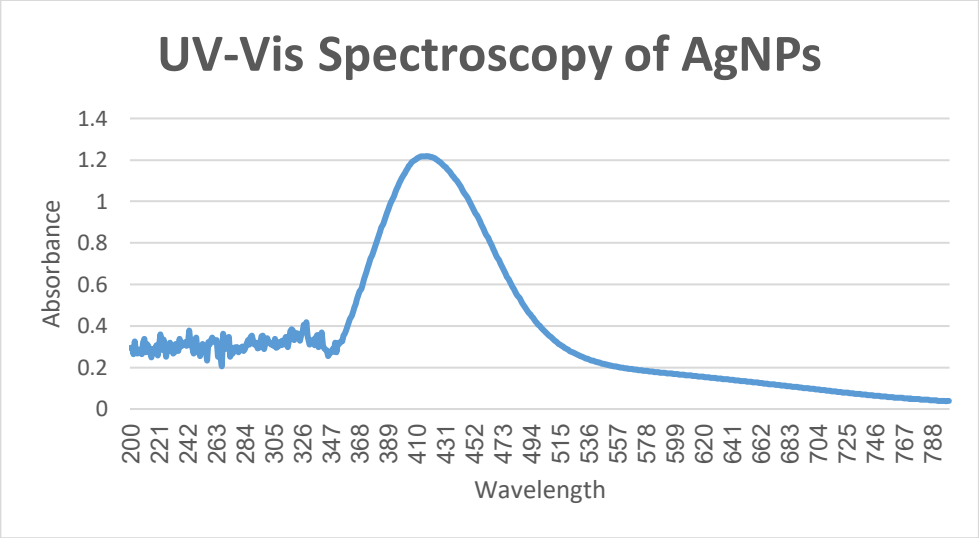

Figure 4.3. UV-vis spectrum of the silver nanoparticles synthesized by Microbacterium sp. H37-C3

The SEM analysis of the synthesized silver nanoparticles was conducted at different magnifications. The SEM images clearly demonstrate the presence of the synthesized nanoparticles. The nanoparticles were observed to have oval and spherical shapes. The particle size distribution ranged from 15 to 30 nm, indicating a relatively uniform size range among the nanoparticles.

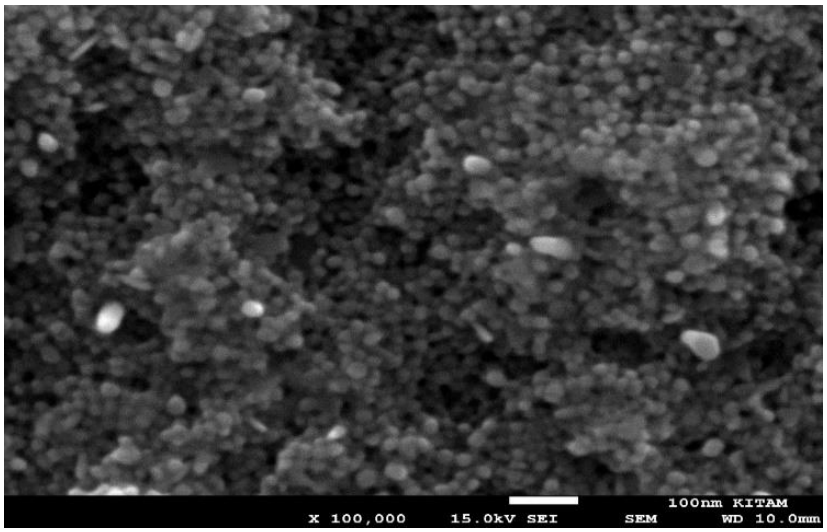

Figure 4.4. SEM image of the silver nanoparticles synthesized by Microbacterium sp. H37-C3

The energy dispersive spectrum (EDX) analysis of the synthesized nanoparticles confirmed the presence of an elemental silver signal, indicating the

presence of silver nanoparticles. Notably, silver nanoparticles exhibit a characteristic strong signal peak at around 3 keV, which is related to the surface plasmon resonance effect. Additionally, the EDX spectrum reveals the presence of other elements such as S, Si, and Cl, as indicated in Figure 4.5.

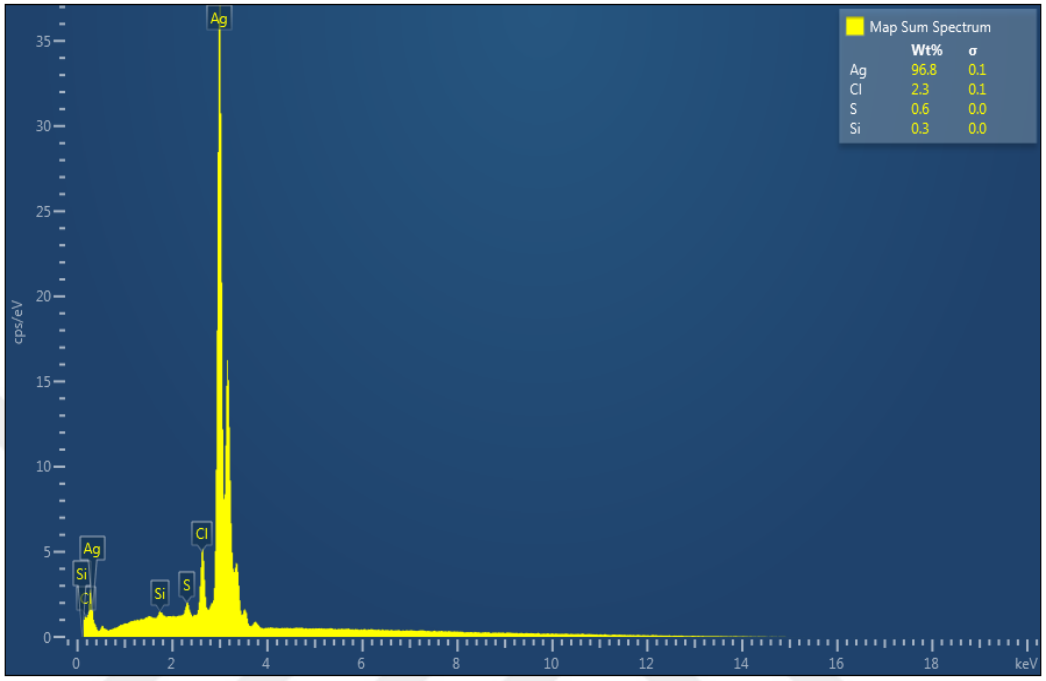

Figure 4.5. The EDX spectrum of the silver nanoparticles synthesized by *Microbacterium* sp. H37-C3

The crystalline structure of the nanoparticles synthesized by *Microbacterium* sp. H37-C3 was revealed by X-ray diffraction analysis. The diffraction peaks were observed at 2θ = 38.152°(Ag2O), 44.247° (Ag/AgO), 64.545° (Ag2O), 77.521° (Ag), and 81.44° and can be indexed to (1 1 1), (2 0 0), (2 2 0), (3 1 1), and (2 2 2) planes of pure silver ions indicating the biosynthesis of silver nanoparticles. High intensity at 38.152° reflection indicates that the crystallites are mainly orients in this plane.

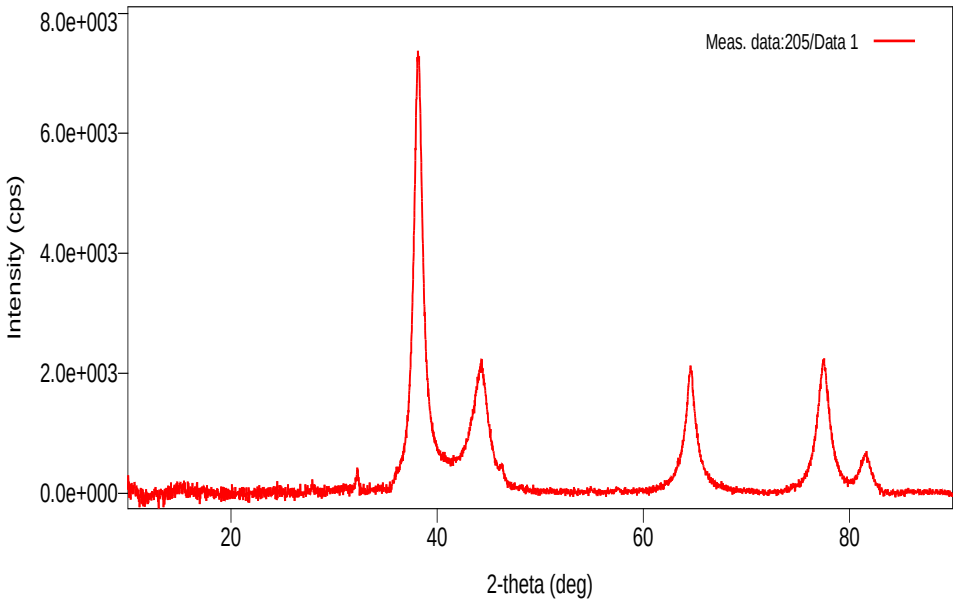

Figure 4.6. The XRD pattern of the silver nanoparticles synthesized by *Microbacterium* sp. H37-C3

4.3. Genome Analysis of *Microbacterium* sp. H37-C3

TYGS, also known as the Type (Strain) Genome Server, is a user-friendly web server designed for genome-based prokaryote taxonomy. It is linked to a huge database that is constantly growing and contains detailed genomic, taxonomic, and nomenclatural data. The server utilizes this wealth of data to infer genome-scale phylogenies and provides advanced estimations for species and subspecies boundaries. These estimations are based on user-defined inputs as well as automatically determined closest-type genome sequences, ensuring accurate and up-to-date taxonomic classification. The TYGS web server serves as a valuable resource for researchers, offering efficient and reliable tools for analyzing and classifying prokaryotic organisms based on their genomes (Meier-Kolthoff and Göker, 2019). The G+C content, an important taxonomic indicator in the genomic domain, plays a significant role in determining affiliations to different species. If the difference in G+C content between genome sequences exceeds 1%, it suggests distinct species associations.

The phylogenetic analysis based on whole-genome comparison on the TYGS server revealed that strain H37-C3 is representative of a novel species within the genus *Microbacterium*. As shown in the phylogenomic tree (Figure 4.7), strain H37-

C3 exhibited a close relationship with *Microbacterium arborescens* DSM 20754. The tree's structure indicates a high degree of genetic similarity and shared ancestry between these two strains within the *Microbacterium* genus. The branch lengths in the tree are scaled based on the GBDP distance formula d5, indicating the genetic distances between the taxa. The numbers above the branches represent GBDP pseudo-bootstrap support values obtained from 100 replications, providing an assessment of the robustness and reliability of the branching patterns in the tree.

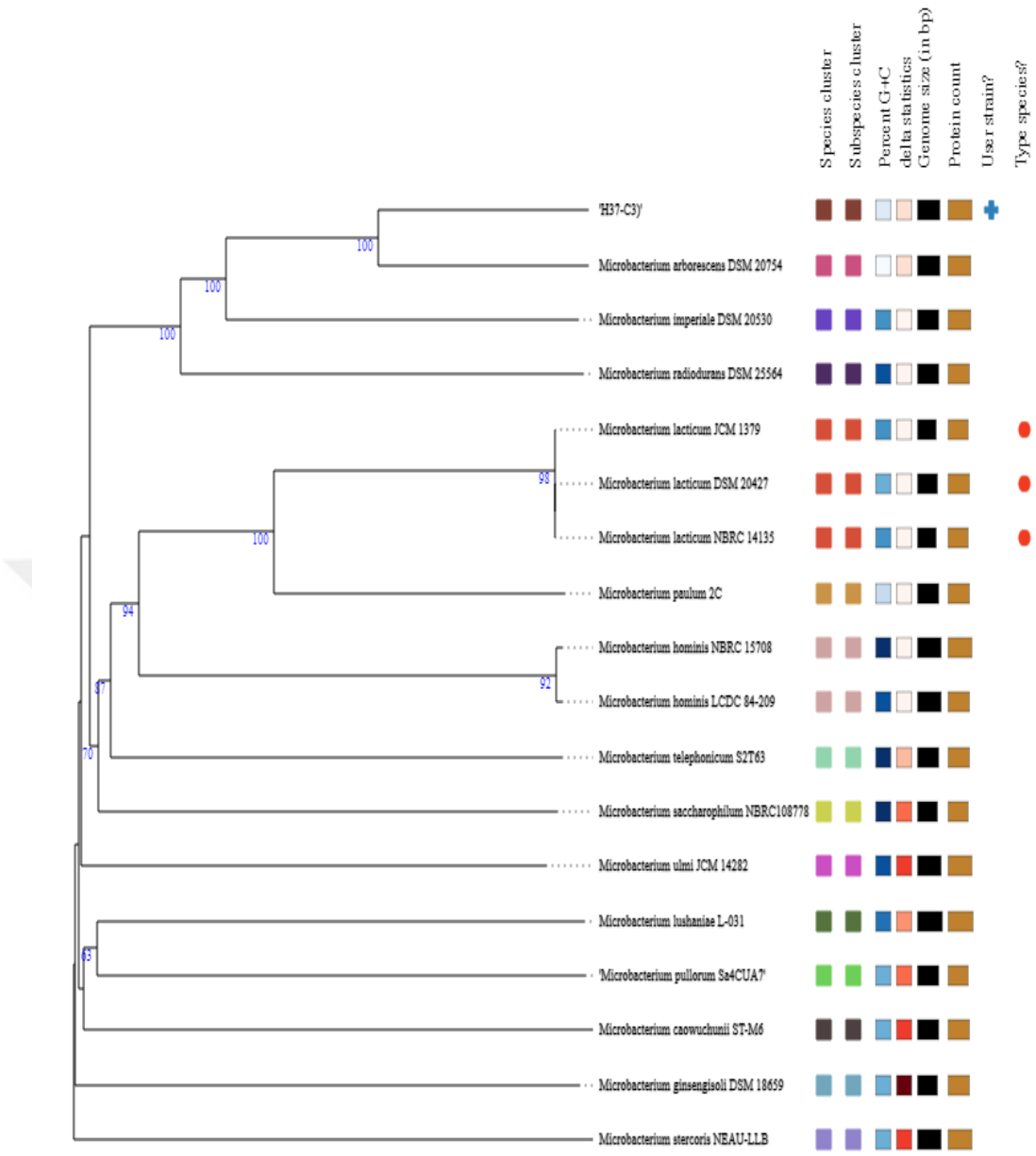

Figure 4.7. The phylogenomic tree constructed on TYGS, representing strain H37-C3 along with other Microbacterium species.

According to the antiSMASH server analysis, (https://antismash.secondarymetabolites.org/#!/start), the genome of *Microbacterium* sp. H37-C3 contains six biosynthetic gene clusters associated with the synthesis of different secondary metabolites. These clusters include two type-III polyketides, a terpene, a beta-lactone lanthipeptide, and a thiopeptide. These gene clusters suggest the potential of *Microbacterium* sp. H37-C3 produces various secondary metabolites, each with its unique biosynthetic pathway and potential bioactive properties (Figure 4.8).

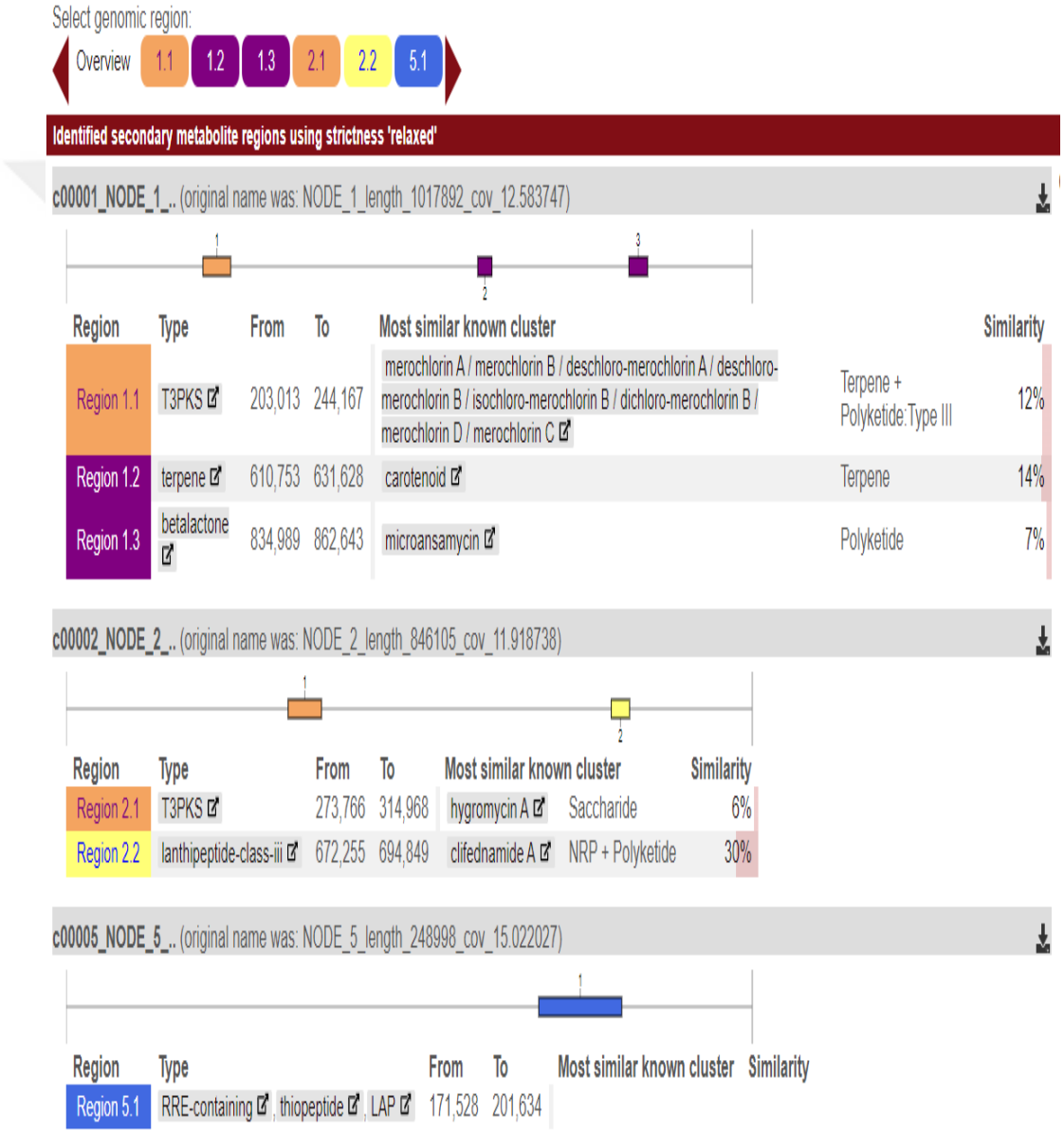

Figure 4.8. Secondary metabolite-coding gene clusters identified in the genome of *Microbacterium* sp. H37-C3

4.4. Antimicrobial Activity of Silver Nanoparticles against *Candida albicans*

The antimicrobial activity and minimum inhibition concentration was determined by employing a modified agar dilution method. The MIC value of the silver nanoparticles against *C. albicans* was determined as 0.25 mg/ml. A concentration of MIC_{10} was used to expose *C. albicans* culture for transcriptomic analysis.

4.5. RNA-Seq Analysis

4.5.1. Raw Data Statistics

Transcriptome sequencing was performed by the Macrogen Inc. (South Korea) using Illumina paired-end sequencing with TruSeq Stranded Total RNA (NEB Microbe) library type. The library size was checked by running the templates on an Agilent Technologies 2100 Bioanalyzer using a DNA 1000 chip. The accurate quantification of DNA library templates was acquired using qPCR according to the Illumina qPCR Quantification Protocol Guide. The RNA concentration of the control group (CA) was calculated as 21.5 ng/µl with average size of 328 bp (Figure 4.9), while the concentration and average size for the CA-Nano were calculated as 30.9 ng/µl and 317 bp, respectively (Figure 4.10).

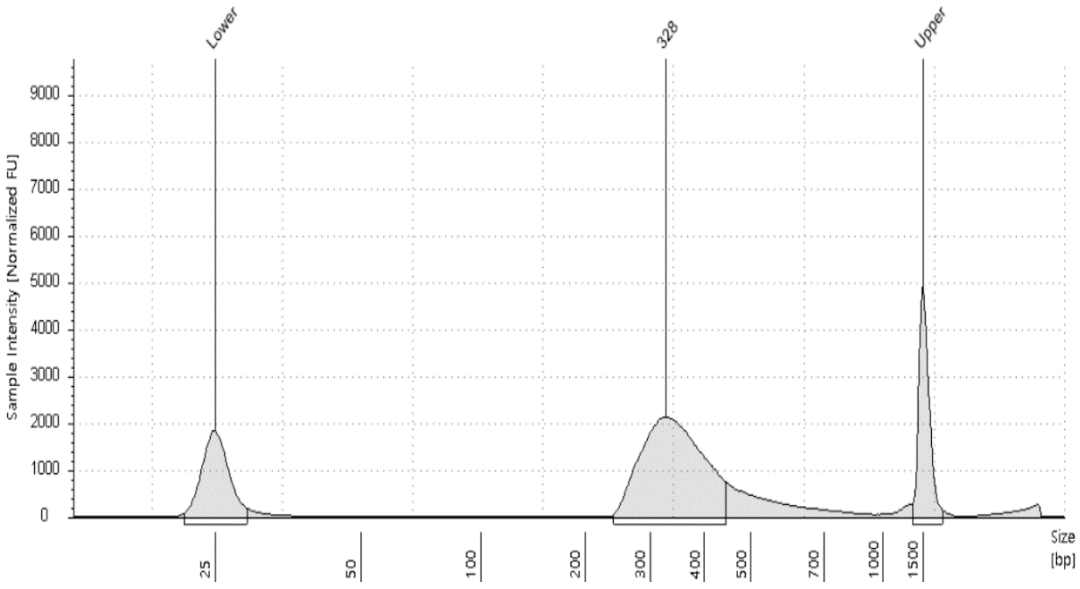

Figure 4.9. Library sample intensity of the control group (CA)

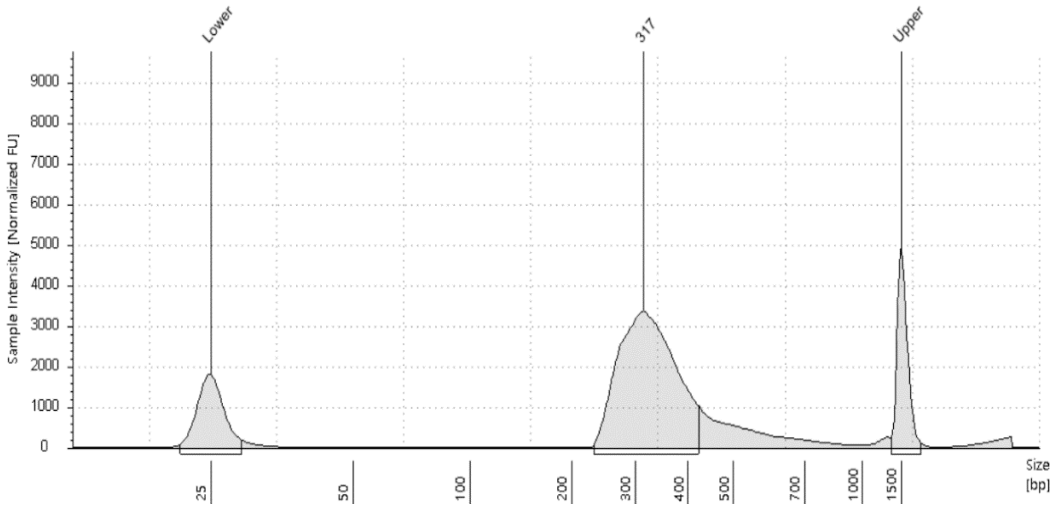

Figure 4.10. Library sample intensity of the AgNP-exposed group (CA-Nano)

The sequencing was performed on Illumina NovaSeq 6000. The total number of bases, reads, GC (%), Q20 (%), and Q30 (%) were calculated for CA and CA-Nano samples (Table 4.1).

Table 4.1. Raw *data* statistics for the control (CA) and AgNP-exposed (CA-Nano) groups

Sample ID	**Total bases(bp)**	**Total reads**	**GC(%)**	**AT(%)**	**Q20(%)**	**Q30(%)**
CA	9,043,539,798	89,539,998	45.5	54.5	98.7	96.0
CA-Nano	8,242,795,840	81,611,840	46.5	53.5	98.7	96.0

· Total bases(bp): Total number of bases sequenced.

· Total reads: Total number of reads. For illumina paired-end sequencing, this value refers to the sum of read1 and read2.

· GC (%): Ratio of GC content.

· AT (%): Ratio of AT content.

· Q20 (%): Ratio of bases that have phred quality score of over 20.

· Q30 (%): Ratio of bases that have phred quality score of over 30.

4.5.2. Alignment and Assembly of the Transcripts

After the quality control of the reads, the fastq files were processed using Trimmomatic tool to remove low-quality reads and adapter sequences. For the control sample, 35420 reads were removed while 32947 reads were dropped for CA-Nano sample (Figures 4.11.).

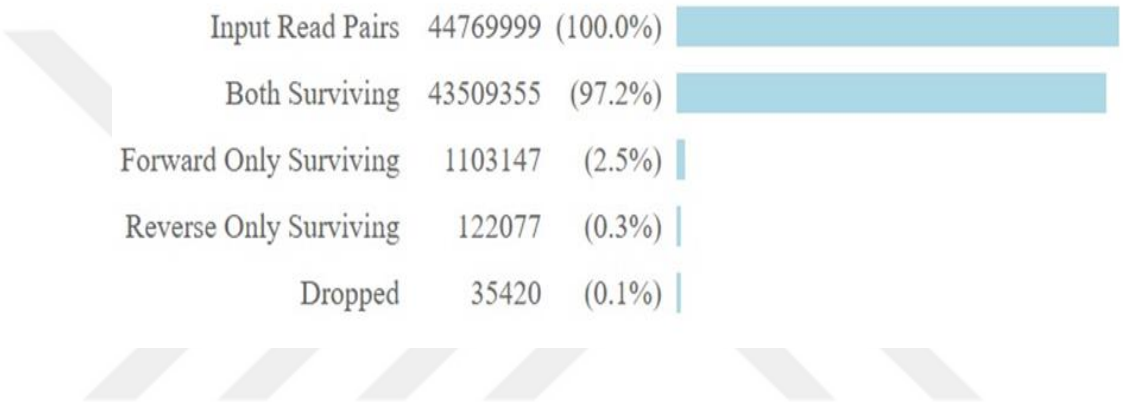

Figure 4.11. Trimmomatic analysis result for the control sample (CA)

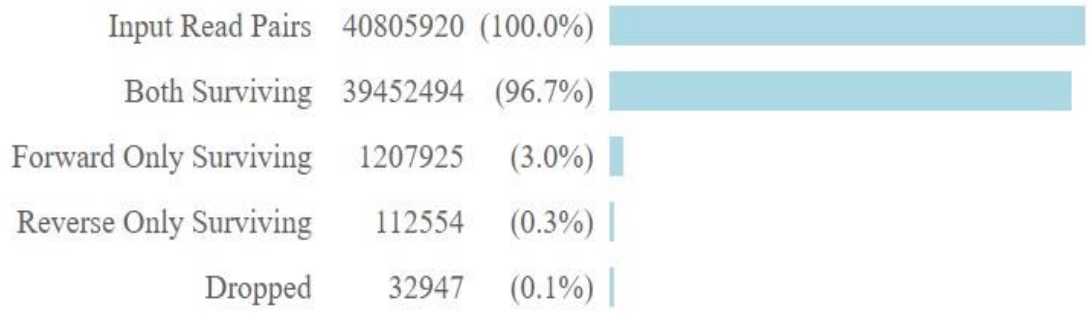

Figure 4.12. Trimmomatic analysis result for the AgNP-exposed sample (CA-Nano)

Using *C. albicans'* reference genome as a reference, the trimmed reads were aligned by using TopHat2 algorithm. A total of 146,734,827 reads were mapped with mean sample mapping quality of 49.43%. The mean sample coverage was 997.39 and mean sample insert size was 164.5 bp (Figures 4.13.).

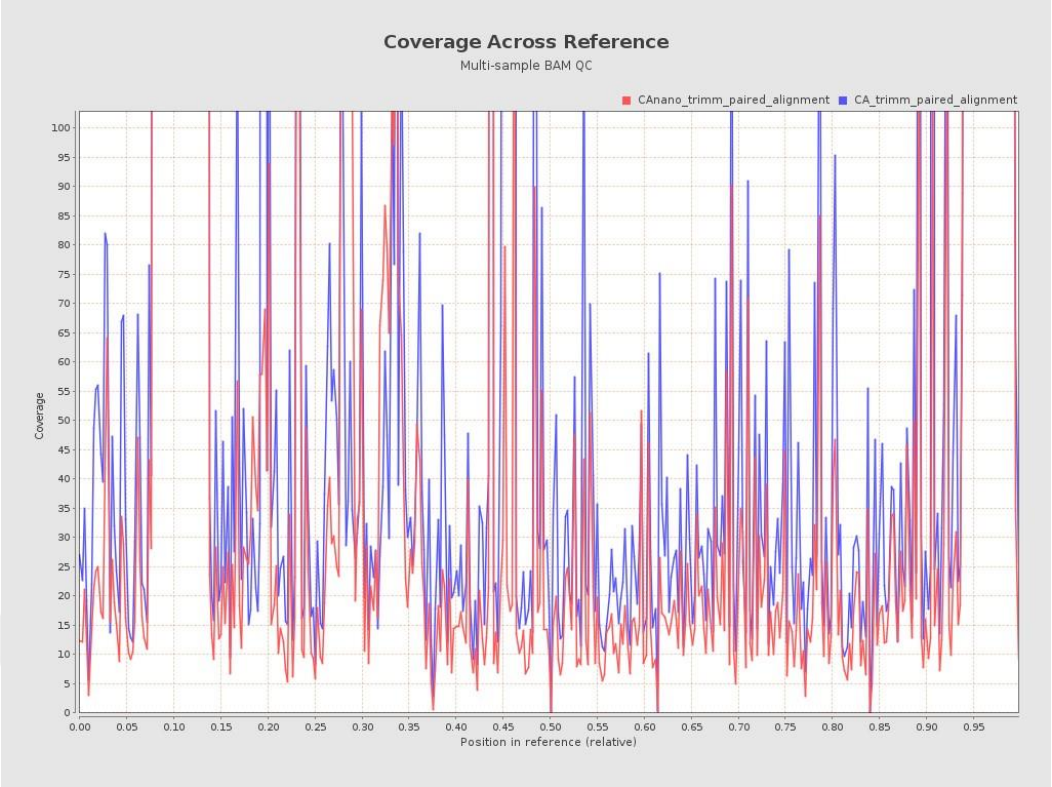

Figure 4.13 The coverage of the reads across the reference genome of *C. albicans*

The mean coverage values across the reference genome of *C. albicans* for CA and CA-Nano samples were calculated as 1006.9 and 987.7, respectively

The mapped reads GC-content of the samples CA and CA-Nano was calculated as 46.06% and 47.03%, respectively (Figure 4.14.)

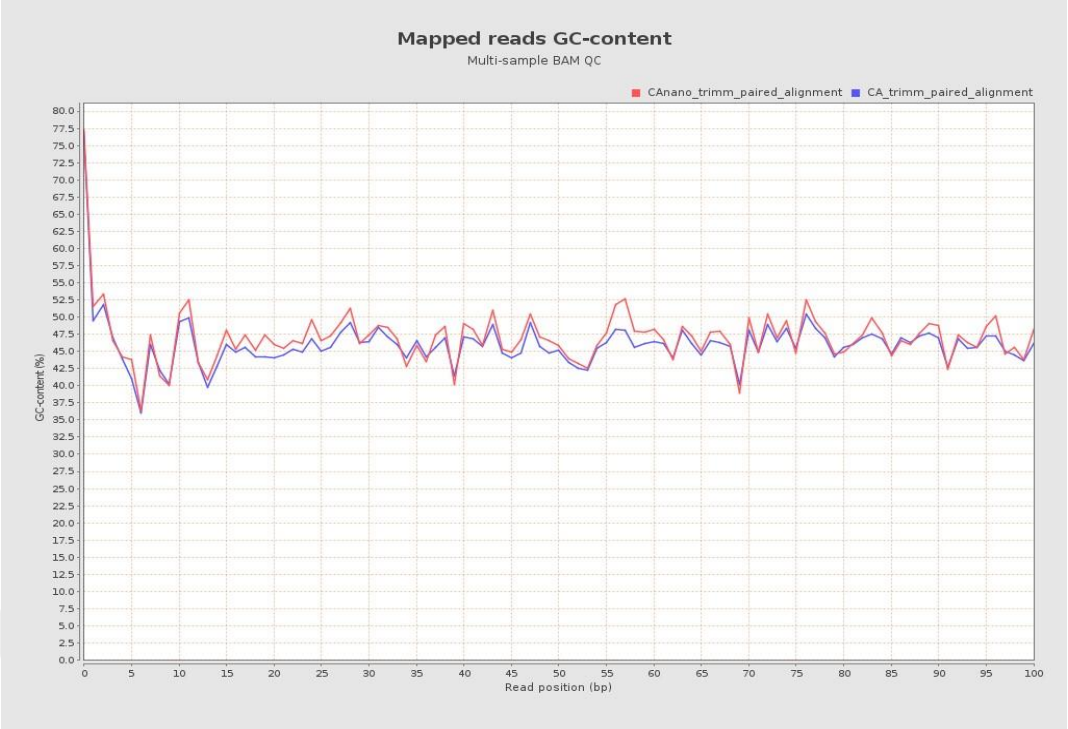

Figure 4.14. Mapped reads GC-content of the samples CA and CA-Nano

The mapping quality mean values for CA and CA-Nano were 49.38 and 49.46, respectively (Figure 4.15.)

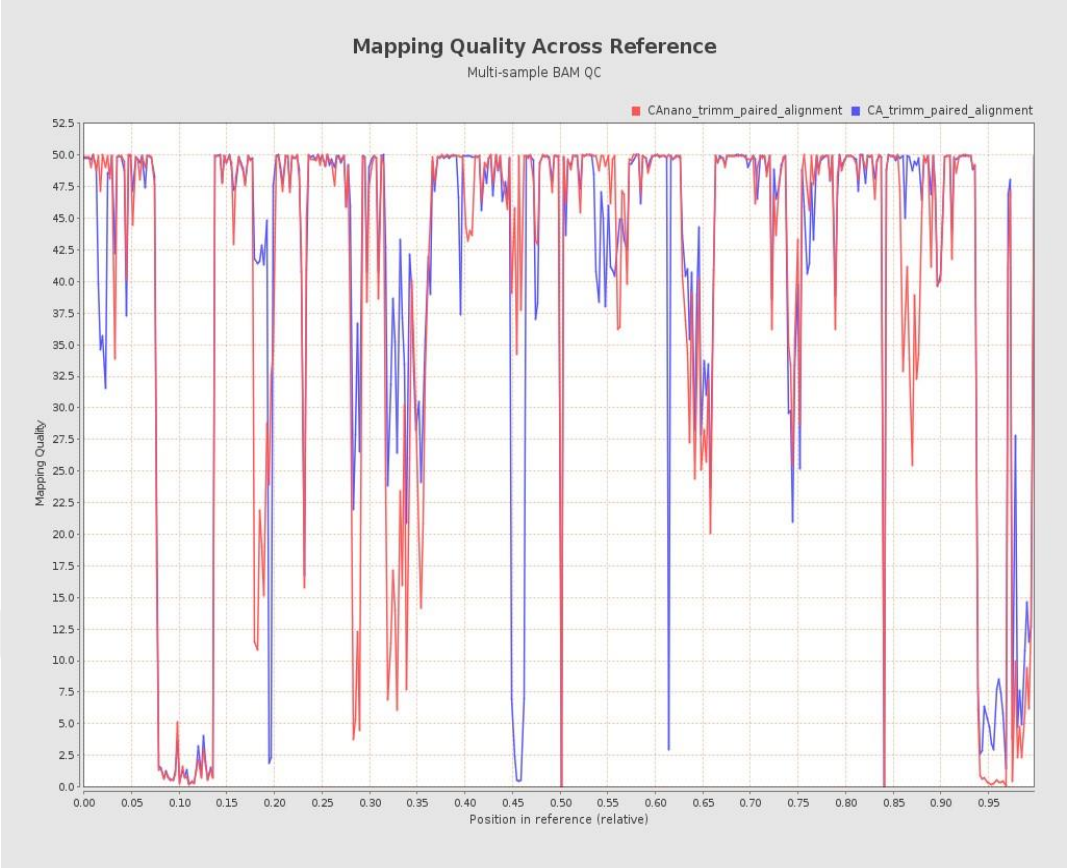

Figure 4.15. The mapping quality of the reads across the reference genome of *C. Albicans*

The insert size median was calculated as 170 and 159 bp for the samples CA and CA-Nano, respectively (Figure 4.16.).

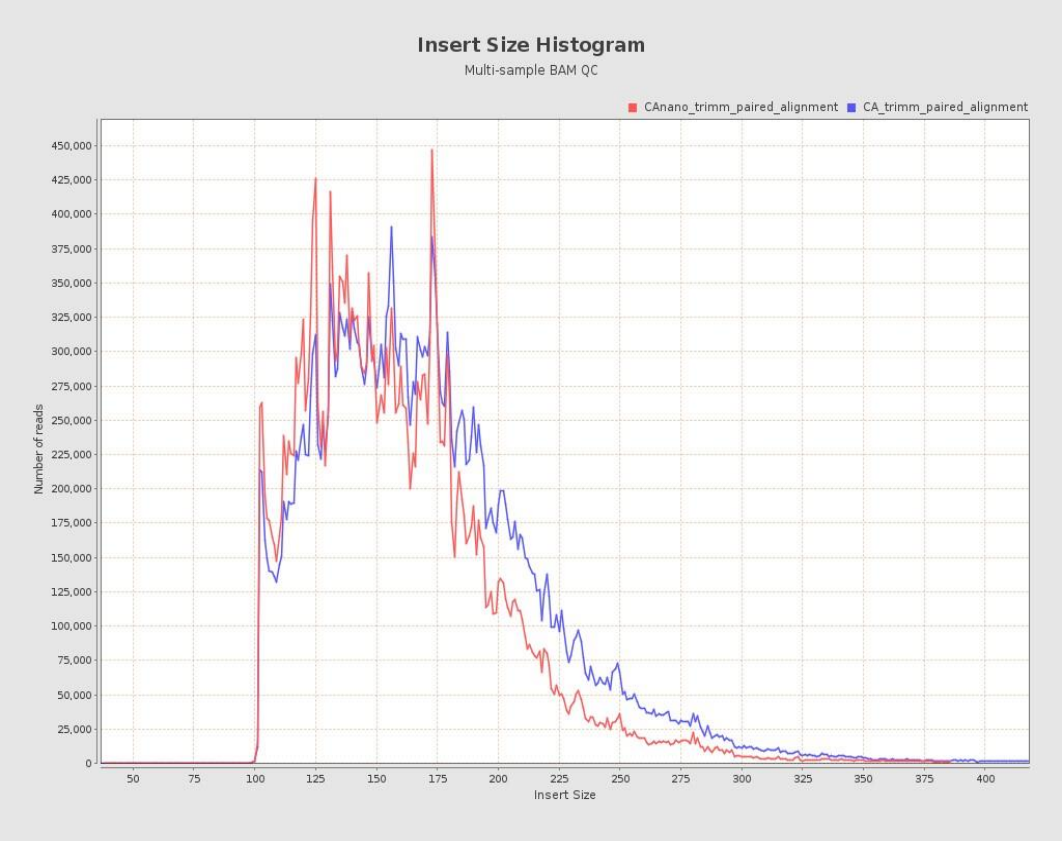

Figure 4.16. The histogram for the insert size distribution

The aligned transcripts were assembled using Cufflinks algorithm to generate expression objects for each sample and the expression set for the samples. The relative abundances of the assembled transcripts were visualized in the histograms. The Cufflinks tool also provided the normalized expression matrices which contain the abundance of each transcript expressed in fragments per kilobase of exon per million fragments mapped (FPKM) and transcripts per million (TPM). The FPKM Histogram tab in the Cufflinks table displays the abundance of normalized gene expression value log2(FPKM+1) (Figure 4.17.) (Figure 4.19.) whereas the TPM Histogram tab displays the abundance of normalized gene expression value log2(TPM+1) (Figure 4.18.) (Figure 4.20.).

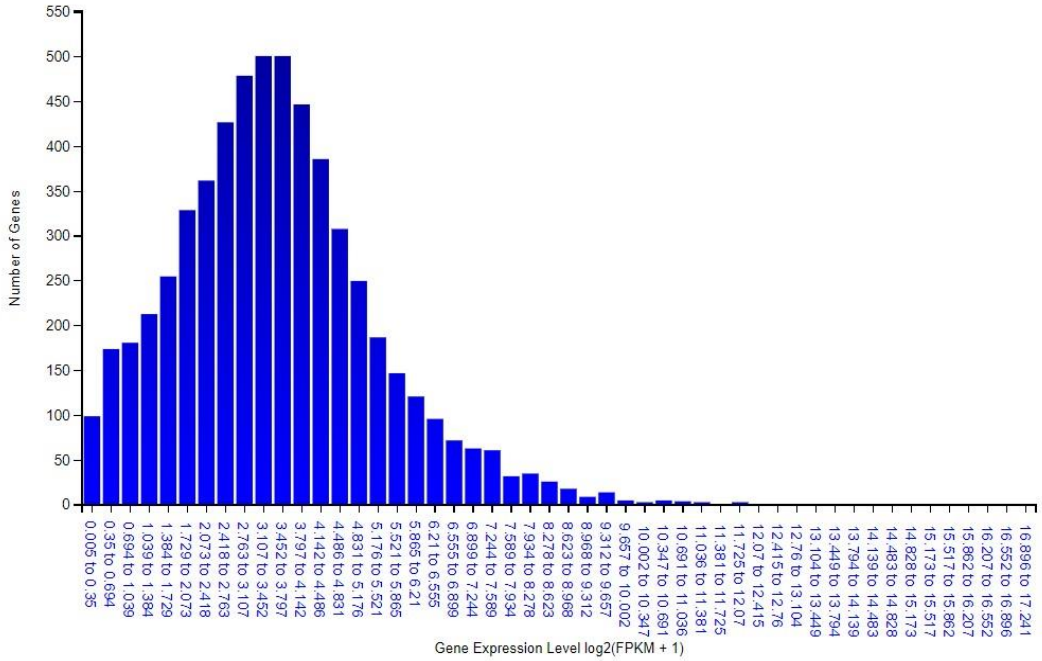

Figure 4.17. The histogram for the fragments per kilobase of exon per million fragments mapped (FPKM) for the control sample (CA)

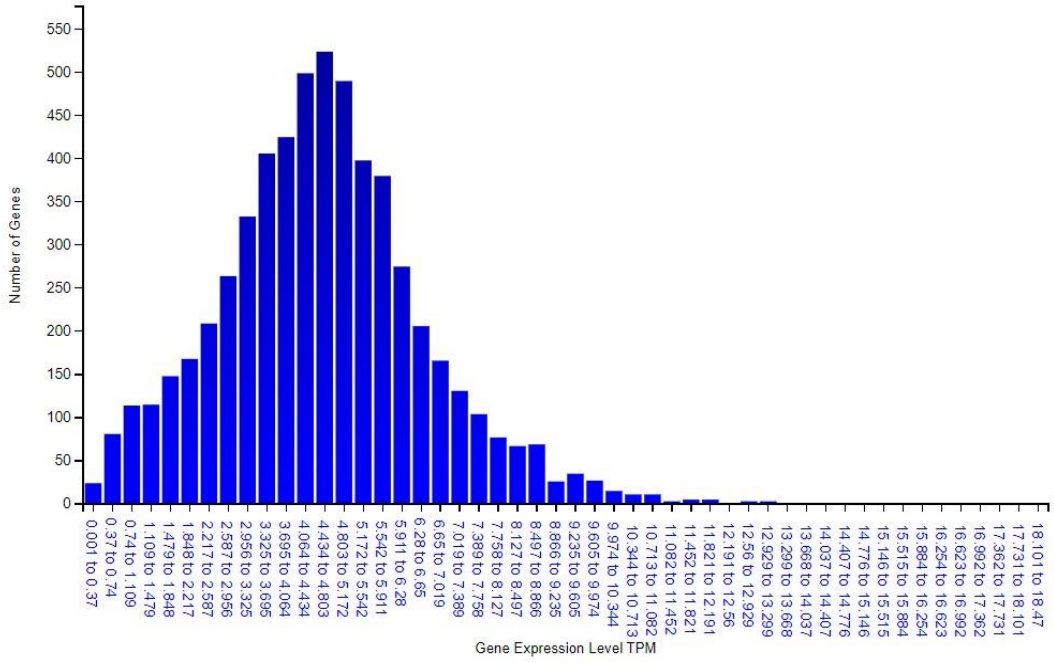

Figure 4.18. The histogram for the transcripts per million (TPM) for the control sample (CA)

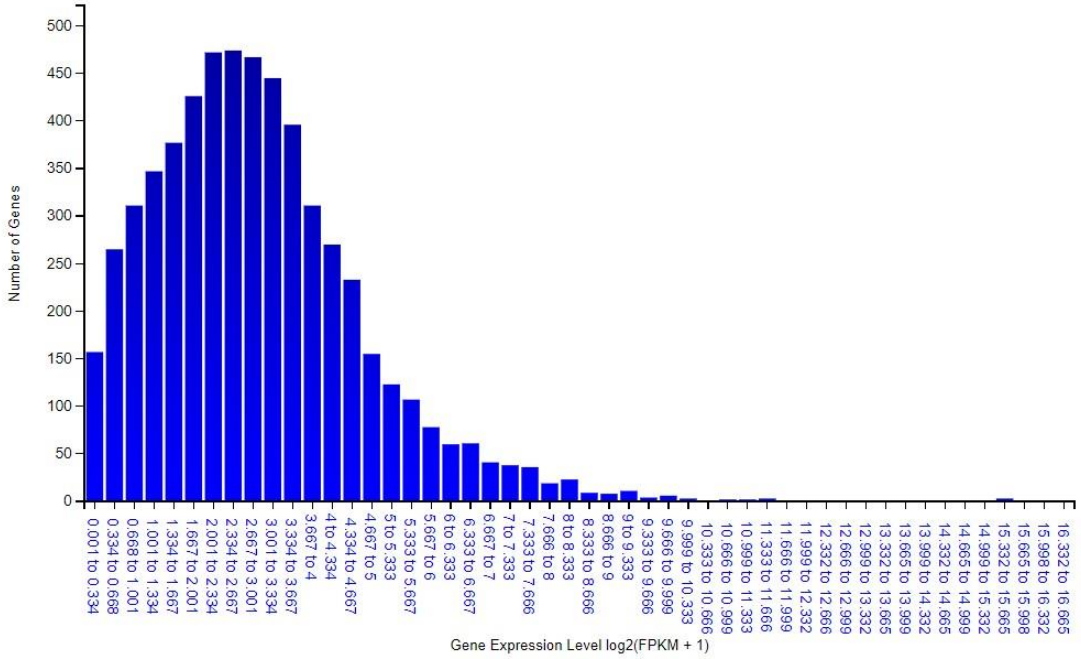

Figure 4.19. The histogram for the fragments per kilobase of exon per million fragments mapped (FPKM) for the AgNP-exposed sample (CA-Nano)

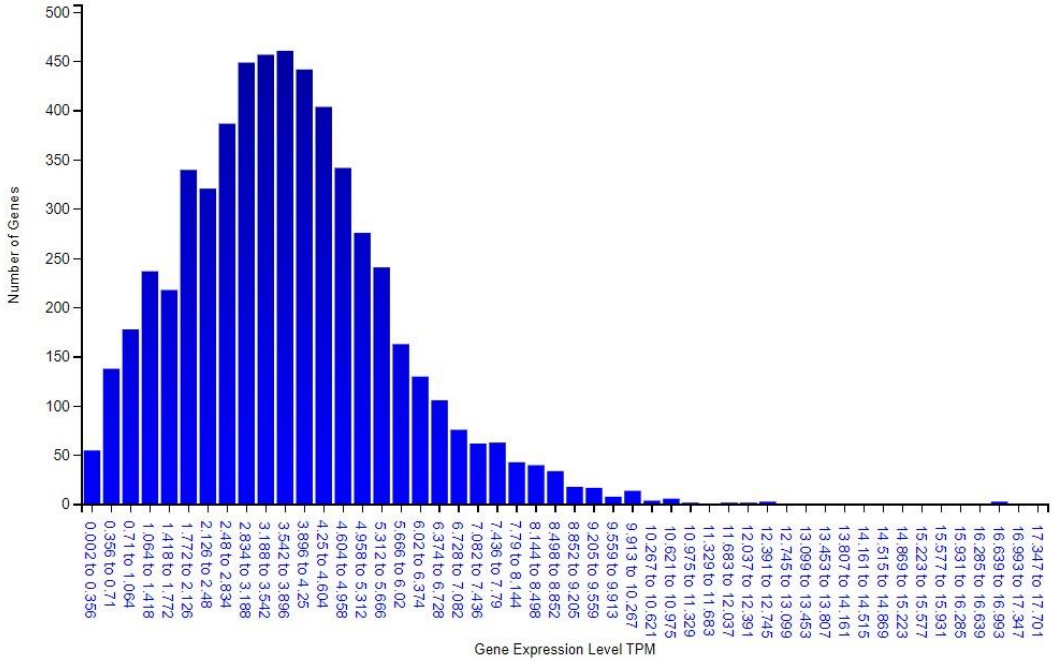

Figure 4.20. The histogram for the transcripts per million (TPM) for the AgNP-exposed sample (CA-Nano)

To determine the differentially expressed genes for the samples CA and CA-Nano, Cuffdiff tool, which calculates the expression in the samples and tests the statistical significance of each observed change in expression between the samples, was employed. No statistically significant change in the expression of any genes was

observed between the samples CA and CA-Nano. However, the expression of several genes was increased by the nanoparticle treatment of C. albicans cells. The expression of the gene coding for a C/D box small nuclear RNA (snoRNA) was observed to be increased by the AgNP treatment. In addition, the CAALFM_C700370WA gene coding for a predicted role in sister chromatid cohesion and telomere length maintenance was upregulated in CA-Nano sample. Another non-coding RNA, which is highly conserved U2 small nuclear RNA involved in splicing coded by CAALFM_C204070CA was also upregulated by the AgNP treatment. The expression of the gene (CAALFM_C205930WA) coding for a cytochrome c oxidase subunit VIIa was also increased compared to the control group. On the other hand, several other C/D box small nucleolar RNA (snoRNA) genes were suppressed by the AgNP treatment. Also, the expression of the gene CAALFM_C110130WA coding for an H/ACA box small nucleolar RNA (snoRNA) was repressed in the CA-Nano sample

5. CONCLUSION

The present study confirmed the green synthesis and antimicrobial properties of AgNPs synthesized by an Antarctic actinobacterium *Microbacterium* sp. H37-C3. In comparison to the nanoparticles produced using chemical and physical methods, biologically produced nanoparticles are considered to be more environmentally friendly. The nanoparticles synthesized by actinobacteria have also additional advantages such as having bioactivities against pathogenic bacteria and fungi. This study also confirmed the antimicrobial activity of silver nanoparticles synthesized by *Microbacterium* sp. H37-C3 against *C. albicans.* The physicochemical characterizations of the AgNPs confirmed that the synthesized nanoparticles are in nanoscale and have crystalline structure.

Transcriptomic analyses have provided insight into toxicity mechanisms of nanoparticles on the microbial cells. *Candida albicans* cells were exposed to AgNPs, and RNA-Seq analysis was used to find the genes that were differentially expressed. Although the observed differences were not significant statistically, several genes responsible for regulation of gene expression, particularly small nucleolar RNAs, were affected by the silver nanoparticle exposure. The low level of expression difference between the control and the AgNP-exposed group might be related to the concentration of the silver nanoparticles (MIC10) used in the present study. Higher levels of the silver nanoparticles could affect the gene expression levels more drastically.

In conclusion, the present study provides insight into biological synthesis of silver nanoparticles by using an Antarctic bacterium as well as possible molecular mechanisms for toxicity of silver nanoparticles on eukaryotic cells.

REFERENCES

Abdel-Hafez, S. I. I., Nafady, N. A., Abdel-Rahim, I. R., Shaltout, A. M., & Mohamed, M. A. (2016). Biogenesis and Optimisation of Silver Nanoparticles by the Endophytic Fungus Cladosporium sphaerospermum. International Journal of Nanomaterials and Chemistry (Online), 2(1), 11–19.

Ahmed, M. N., Rao, T., Saeed, A., Mutahir, Z., Hameed, S., Inayat, S., . . . Ahmed, S. (2021). Antifungal Drugs: Mechanism of Action and Resistance. In Springer eBooks (pp. 143–165).

Aird, D., Ross, M. W., Chen, W., Danielsson, M., Fennell, T. R., Russ, C., . . . Gnirke, A. (2011). Analyzing and minimizing PCR amplification bias in Illumina sequencing libraries. GenomeBiology.com (London. Print), 12(2), R18.

Albertson, G. D., Niimi, M., Cannon, R. D., & Jenkinson, H. F. (1996). Multiple efflux mechanisms are involved in Candida albicans fluconazole resistance. Antimicrobial Agents and Chemotherapy, 40(12), 2835–2841.

Argimón, S., Wishart, J. A., Leng, R. P., MacAskill, S., Mavor, A., Alexandris, T., . . . Brown, A. J. P. (2007). Developmental Regulation of an Adhesin Gene during Cellular Morphogenesis in the Fungal Pathogen Candida albicans. Eukaryotic Cell, 6(4), 682–692.

Arkin, A. P., Cottingham, R. W., Henry, C. D., Harris, N. L., Stevens, R., Maslov, S., . . . Yu, D. (2018). KBase: The United States Department of Energy Systems Biology Knowledgebase. Nature Biotechnology, 36(7), 566–569.

Balashov, S., Park, S. I., & Perlin, D. S. (2006). Assessing Resistance to the Echinocandin Antifungal Drug Caspofungin in Candida albicans by Profiling Mutations in FKS1. Antimicrobial Agents and Chemotherapy, 50(6), 2058–2063.

Bhattacharya, S., Sae-Tia, S., & Fries, B. C. (2020). Candidiasis and Mechanisms of Antifungal Resistance. Antibiotics, 9(6), 312.

Bhattacharya, S., Sobel, J. D., & White, T. C. (2016a). A Combination Fluorescence Assay Demonstrates Increased Efflux Pump Activity as a Resistance Mechanism in Azole-Resistant Vaginal Candida albicans Isolates. Antimicrobial Agents and Chemotherapy, 60(10), 5858–5866.

Bhattacharya, S., Sobel, J. D., & White, T. C. (2016b). A Combination Fluorescence Assay Demonstrates Increased Efflux Pump Activity as a Resistance Mechanism in Azole-Resistant Vaginal Candida albicans Isolates. Antimicrobial Agents and Chemotherapy, 60(10), 5858–5866.

Blin, K., Shaw, S., Augustijn, H. E., Reitz, Z. L., Biermann, F., Alanjary, M., . . . Weber, T. (2023). antiSMASH 7.0: new and improved predictions for detection, regulation, chemical structures and visualisation. PubMed.

Blin, K., Shaw, S., Kloosterman, A. M., Charlop-Powers, Z., Van Wezel, G. P., Medema, M. H., & Weber, T. (2021a). antiSMASH 6.0: improving cluster detection and comparison capabilities. Nucleic Acids Research, 49(W1), W29–W35.

Blin, K., Shaw, S., Kloosterman, A. M., Charlop-Powers, Z., Van Wezel, G. P., Medema, M. H., & Weber, T. (2021b). antiSMASH 6.0: improving cluster detection and comparison capabilities. Nucleic Acids Research, 49(W1), W29–W35.

Bolger, A., Lohse, M., & Usadel, B. (2014). Trimmomatic: a flexible trimmer for Illumina sequence data. Bioinformatics, 30(15), 2114–2120.

Casadevall, A. (2007). Determinants of virulence in the pathogenic fungi. Fungal Biology Reviews, 21(4), 130–132.

Costa-De-Oliveira, S., & Rodrigues, A. G. (2020). Candida albicans Antifungal Resistance and Tolerance in Bloodstream Infections: The Triad Yeast-Host-Antifungal. Microorganisms, 8(2), 154.

Costa-Silva, J., Domingues, D. S., Menotti, D., Hungria, M., & Lopes, F. M. (2023). Temporal progress of gene expression analysis with RNA-Seq data: A review on the relationship between computational methods. Computational and Structural Biotechnology, 21, 86–98.

De Simeis, D., & Serra, S. (2021). Actinomycetes: A Never-Ending Source of Bioactive Compounds—An Overview on Antibiotics Production. Antibiotics, 10(5), 483.

Dong, Z., Rao, M. P. N., Xiao, M., Wang, H., Hozzein, W. N., Chen, W., & Li, W. (2017). Antibacterial Activity of Silver Nanoparticles against Staphylococcus warneri Synthesized Using Endophytic Bacteria by Photo-irradiation. Frontiers in Microbiology, 8.

Du, R., Zhao, F., Peng, Q., & Zhou, Z. (2018). Production and characterization of bacterial cellulose produced by Gluconacetobacter xylinus isolated from Chinese persimmon vinegar. Carbohydrate Polymers, 194, 200–207.

Dutta, P. K., Kumari, J., Borah, P., Baruah, P., Kaman, P. K., Das, G., . . . Saikia, B. (2020). Synthesis of fungus mediate silver nanoparticles (AgNP) its characterization and study the efficacy against inoculam, biomass and protein content of Fusarium oxysporum. International Journal of Chemical Studies, 8(4), 2619–2625.

El-Bendary, M. A., Afifi, S. S., Moharam, M. E., El-Ola, S. M. A., Salama, A., Omara, E. A., . . . Gawdat, N. A. (2020). Biosynthesis of silver nanoparticles using isolated Bacillus subtilis: characterization, antimicrobial activity, cytotoxicity, and their performance as antimicrobial agent for textile materials. Preparative Biochemistry & Biotechnology, 51(1), 54–68.

Finotello, F., & Di Camillo, B. (2014). Measuring differential gene expression with RNA-seq: challenges and strategies for data analysis. Briefings in Functional Genomics, 14(2), 130–142.

Griebel, T., Zacher, B., Ribeca, P., Raineri, E., Lacroix, V., Guigó, R., & Sammeth, M. (2012). Modelling and simulating generic RNA-Seq experiments with the flux simulator. Nucleic Acids Research, 40(20), 10073–10083.

Hadjadj, L., Rathored, J., Keita, M. B., Michelle, C., Levasseur, A., Raoult, D., . . . Bittar, F. (2016). Non contiguous-finished genome sequence and description of Microbacterium gorillae sp. nov. Standards in Genomic Sciences, 11(1).

Hardcastle, T. J., & Kelly, K. A. (2010). baySeq: Empirical Bayesian methods for identifying differential expression in sequence count data. BMC Bioinformatics, 11(1).

Haro-Reyes, T., Díaz-Peralta, L., Galván-Hernández, A., Rodríguez-López, A., Rodríguez-Fragoso, L., & Ortega-Blake, I. (2022). Polyene Antibiotics Physical Chemistry and

Their Effect on Lipid Membranes; Impacting Biological Processes and Medical Applications. Membranes, 12(7), 681.

Hatem, A., Bozdağ, D., Toland, A. E., & Çatalyürek, Ü. V. (2013). Benchmarking short sequence mapping tools. BMC Bioinformatics, 14(1).

Huang, Z., Zeng, Z., Song, Z., Chen, A., Zeng, G., Xiao, R., . . . Chen, G. (2020). Antimicrobial efficacy and mechanisms of silver nanoparticles against Phanerochaete chrysosporium in the presence of common electrolytes and humic acid. Journal of Hazardous Materials, 383, 121153.

Jamkhande, P. G., Ghule, N. W., Bamer, A. H., & Kalaskar, M. G. (2019). Metal nanoparticles synthesis: An overview on methods of preparation, advantages and disadvantages, and applications. Journal of Drug Delivery Science and Technology, 53, 101174.

Kanafani, Z. A., & Perfect, J. R. (2008). Resistance to Antifungal Agents: Mechanisms and Clinical Impact. Clinical Infectious Diseases, 46(1), 120–128.

Kim, D., Pertea, G., Trapnell, C., Pimentel, H., Kelley, R., & Salzberg, S. L. (2013). TopHat2: accurate alignment of transcriptomes in the presence of insertions, deletions and gene fusions. GenomeBiology.com (London. Print), 14(4), R36.

Law, C. W., Chen, Y., Shi, W., & Smyth, G. K. (2014). voom: precision weights unlock linear model analysis tools for RNA-seq read counts. GenomeBiology.com (London. Print), 15(2), R29.

Lee, S. Y., & Lee, S. H. (2019). Silver Nanoparticles: Synthesis and Application for Nanomedicine. International Journal of Molecular Sciences, 20(4), 865.

Lee, Y., Puumala, E., Robbins, N., & Cowen, L. E. (2020). Antifungal Drug Resistance: Molecular Mechanisms in Candida albicans and Beyond. Chemical Reviews, 121(6), 3390–3411.

Liu, S., Wang, Z., Zhu, R., Wang, F., Cheng, Y., & Liu, Y. (2021). Three Differential Expression Analysis Methods for RNA Sequencing: limma, EdgeR, DESeq2. Journal of Visualized Experiments, (175).

Lo, H., Köhler, J. R., DiDomenico, B., Loebenberg, D., Cacciapuoti, A., & Fink, G. R. (1997). Nonfilamentous C. albicans Mutants Are Avirulent. Cell, 90(5), 939–949.

Love, M. I., Huber, W., & Anders, S. (2014). Moderated estimation of fold change and dispersion for RNA-seq data with DESeq2. Genome Biology, 15(12).

Manivasagan, P., Venkatesan, J., Sivakumar, K., & Kim, S. (2014). Actinobacteria mediated synthesis of nanoparticles and their biological properties: A review. Critical Reviews in Microbiology, 1–13.

Marichal, P., Koymans, L., Willemsens, S., Bellens, D., Verhasselt, P., Luyten, W., . . . Vanden Bossche, H. (1999). Contribution of mutations in the cytochrome P450 14α-demethylase (Erg11p, Cyp51p) to azole resistance in Candida albicans. Microbiology, 145(10), 2701–2713.

Mayer, F. L., Wilson, D., & Hube, B. (2013). Candida albicanspathogenicity mechanisms. Virulence, 4(2), 119–128.

Meier-Kolthoff, J. P., & Göker, M. (2019a). TYGS is an automated high-throughput platform for state-of-the-art genome-based taxonomy. Nature Communications, 10(1).

Meier-Kolthoff, J. P., & Göker, M. (2019b). TYGS is an automated high-throughput platform for state-of-the-art genome-based taxonomy. Nature Communications, 10(1).

Nailis, H., Kucharíková, S., Řičicová, M., Van Dijck, P., Deforce, D., Nelis, H., & Coenye, T. (2010). Real-time PCR expression profiling of genes encoding potential virulence factors in Candida albicans biofilms: identification of model-dependent and -independent gene expression. BMC Microbiology, 10(1).

Nobile, C. J., & Mitchell, A. P. (2005). Regulation of Cell-Surface Genes and Biofilm Formation by the C. albicans Transcription Factor Bcr1p. Current Biology, 15(12), 1150–1155.

Oshlack, A., Robinson, M. D., & Young, M. R. (2010). From RNA-seq reads to differential expression results. GenomeBiology.com (London. Print), 11(12), 220.

Perlin, D. S. (2011). Current perspectives on echinocandin class drugs. Future Microbiology, 6(4), 441–457.

Robinson, M. D., McCarthy, D. J., & Smyth, G. K. (2009). edgeR: a Bioconductor package for differential expression analysis of digital gene expression data. Bioinformatics, 26(1), 139–140.

Salem, S. S., & Gobouri, A. A. (2020). Green Synthesis of Metallic Nanoparticles and Their Prospective Biotechnological Applications: an Overview. Biological Trace Element Research, 199(1), 344–370.

Sanglard, D., Ischer, F., Monod, M., & Bille, J. (1997). Cloning of Candida albicans genes conferring resistance to azole antifungal agents: characterization of CDR2, a new multidrug ABC transporter gene. Microbiology, 143(2), 405–416.

Sastry, M., Mayya, K. S., & Bandyopadhyay, K. (1997). pH Dependent changes in the optical properties of carboxylic acid derivatized silver colloidal particles. Colloids and Surfaces A: Physicochemical and Engineering Aspects, 127(1–3), 221–228.

Satiman, E. a. F. E. N., Ahmad, H., Ramzi, A. B., Wahab, R. A., Kaderi, M. A., Harun, W. S. W., . . . Arzmi, M. H. (2020). The role ofCandida albicanscandidalysinECE1gene in oral carcinogenesis. Journal of Oral Pathology &Amp; Medicine, 49(9), 835–841.

Shafiei, M., Peyton, L., Hashemzadeh, M., & Foroumadi, A. (2020). History of the development of antifungal azoles: A review on structures, SAR, and mechanism of action. Bioorganic Chemistry, 104, 104240.

Shendure, J., & Ji, H. (2008). Next-generation DNA sequencing. Nature Biotechnology, 26(10), 1135–1145.

Tarazona, S., Furió-Tarí, P., Turrà, D., Di Pietro, A., Nueda, M. J., Ferrer, A., & Conesa, A. (2015). Data quality aware analysis of differential expression in RNA-seq with NOISeq R/Bioc package. Nucleic Acids Research, gkv711.

Tarazona, S., Garcia-Alcalde, F., Dopazo, J., Ferrer, A., & Conesa, A. (2011). Differential expression in RNA-seq: A matter of depth. Genome Research, 21(12), 2213–2223.

Toda, M., Williams, S. R., Berkow, E. L., Farley, M. M., Harrison, L. H., Bonner, L., . . . Vallabhaneni, S. (2019). Population-Based Active Surveillance for Culture-Confirmed Candidemia — Four Sites, United States, 2012–2016. Morbidity and Mortality Weekly Report, 68(8), 1–15.

Trapnell, C., Williams, B. G., Pertea, G., Mortazavi, A., Kwan, G., Van Baren, M. J., . . . Pachter, L. (2010). Transcript assembly and quantification by RNA-Seq reveals unannotated transcripts and isoform switching during cell differentiation. Nature Biotechnology, 28(5), 511–515.

Vandeputte, P., Ferrari, S., & Coste, A. T. (2012). Antifungal Resistance and New Strategies to Control Fungal Infections. International Journal of Microbiology, 2012, 1–26.

Veen, M., Stahl, U., & Lang, C. (2003). Combined overexpression of genes of the ergosterol biosynthetic pathway leads to accumulation of sterols in. Fems Yeast Research, 4(1), 87–95.

Ventura, M., Canchaya, C., Tauch, A., Chandra, G., Fitzgerald, G. F., Chater, K. F., & Van Sinderen, D. (2007). Genomics of Actinobacteria : Tracing the Evolutionary History of an Ancient Phylum. Microbiology and Molecular Biology Reviews, 71(3), 495–548.

Verma, A., & Mehata, M. S. (2016). Controllable synthesis of silver nanoparticles using Neem leaves and their antimicrobial activity. Journal of Radiation Research and Applied Sciences, 9(1), 109–115.

Wiegand, I., Hilpert, K., & Hancock, R. E. W. (2008). Agar and broth dilution methods to determine the minimal inhibitory concentration (MIC) of antimicrobial substances. Nature Protocols, 3(2), 163–175.

Wypij, M., Czarnecka, J., Świecimska, M., Dahm, H., Rai, M., & Golińska, P. (2018). Synthesis, characterization and evaluation of antimicrobial and cytotoxic activities of biogenic silver nanoparticles synthesized from Streptomyces xinghaiensis OF1 strain. World Journal of Microbiology & Biotechnology, 34(2).

Xiao, Z., Wang, Q., Zhu, F., & An, Y. (2019). Epidemiology, species distribution, antifungal susceptibility and mortality risk factors of candidemia among critically ill patients: a retrospective study from 2011 to 2017 in a teaching hospital in China. Antimicrobial Resistance and Infection Control, 8(1).

Yaqoob, A. A., Umar, K., & Ibrahim, M. N. M. (2020). Silver nanoparticles: various methods of synthesis, size affecting factors and their potential applications–a review. Applied Nanoscience, 10(5), 1369–1378.

CURRICULUM VITEA

Osaid ALHAROUN

BSc: Faculty of pharmacy – Aleppo university 2010. (21.07.2023).

Contact Information :

ORCID ID : 0000-0002-3152-3061

Publications :

1. Alharoun O. , Ay H. Genomic Analysis of Microbacterium sp. H37-C3 Synthesizing Silver Nanoparticles. 5th International Eurasian Conference on Biological and Chemical Sciences, 23-25 November 2022, Ankara, Turkiye (Oral presentation)